# EXPERIMENTAL INVESTIGATION ON RESEARCH OCTANE NUMBER OF LIQUEFIED PETROLEUM GAS

A THESIS SUBMITTED TO
THE GRADUATE SCHOOL OF NATURAL AND APPLIED SCIENCES
OF
MIDDLE EAST TECHNICAL UNIVERSITY

BY

ÖMER TUĞBERK KEÇECİOĞLU

IN PARTIAL FULFILLMENT OF THE REQUIREMENTS
FOR
THE DEGREE OF MASTER OF SCIENCE
IN
MECHANICAL ENGINEERING

NOVEMBER 2019

Approval of the thesis:

**EXPERIMENTAL INVESTIGATION ON RESEARCH OCTANE NUMBER OF LIQUEFIED PETROLEUM GAS**

submitted by **ÖMER TUĞBERK KEÇECİOĞLU** in partial fulfillment of the requirements for the degree of **Master of Science in Mechanical Engineering Department, Middle East Technical University** by,

Prof. Dr. Halil Kalıpçılar
Dean, Graduate School of **Natural and Applied Sciences** _____

Prof. Dr. M.A. Sahir Arıkan
Head of Department, **Mechanical Engineering** _____

Prof. Dr. Ahmet Yozgatlıgil
Supervisor, **Mechanical Engineering, METU** _____

**Examining Committee Members:**

Assoc. Prof. Dr. M. Metin Yavuz
Mechanical Engineering, METU _____

Prof. Dr. Ahmet Yozgatlıgil
Mechanical Engineering, METU _____

Assoc. Prof. Dr. A. Buğra Koku
Mechanical Engineering, METU _____

Assist. Prof. Dr. Feyza Kazanç Özerinç
Mechanical Engineering, METU _____

Assoc. Prof. Dr. Murat Aktaş
Mechanical Engineering, TOBB ETU _____

Date: 26.11.2019

**I hereby declare that all information in this document has been obtained and presented in accordance with academic rules and ethical conduct. I also declare that, as required by these rules and conduct, I have fully cited and referenced all material and results that are not original to this work.**

Name, Surname: Ömer Tuğberk Keçecioğlu

Signature:

# ABSTRACT

## EXPERIMENTAL INVESTIGATION ON RESEARCH OCTANE NUMBER OF LIQUEFIED PETROLEUM GAS

Keçecioğlu, Ömer Tuğberk
Master of Science, Mechanical Engineering
Supervisor: Prof. Dr. Ahmet Yozgatlıgil

November 2019, 86 pages

This research presents an experimental study of the Research Octane Numbers (RON) of Liquefied Petroleum Gas (LPG) using a modified Cooperative Fuel Research Engine which can run with gaseous high-octane fuels. A comprehensive set of RON data for the LPG compositions that contain propane, n-butane, iso-butane and trace amount of olefins are presented. In order to determine RON of the various samples, the bracketing method that is defined for liquid fuels by the American Society for Testing and Materials (ASTM) was followed. A linear empirical model which correlates LPG composition to octane number is then developed. The empirical model is tested using experimental data in the literature in order to observe confidence. Very good agreement with the literature is observed.

**Keywords**: Liquefied Petroleum Gas, LPG, Octane Number, RON, CFR Engine

# ÖZ

## SIVILAŞTIRILMIŞ PETROL GAZI (LPG) ARAŞTIRMA OKTAN SAYISININ DENEYSEL OLARAK İNCELENMESİ

Keçecioğlu, Ömer TuğberkYüksek Lisans, Makina Mühendisliği
Tez Danışmanı: Prof. Dr. Ahmet Yozgatlıgil

Kasım 2019, 86 sayfa

Bu çalışmada Sıvılaştırılmış Petrol Gazının (LPG) Araştırma Oktan Sayısı (RON) modifiye edilmiş, gaz fazındaki yüksek oktanlı yakıtlarla çalışabilen CFR motoru kullanılarak ölçülmüştür. Çeşitli oranlarda propan, n-bütan, iso-bütan ve eser miktarda olefin içeren LPG örnekleriyle kapsamlı bir deney matrisi oluşturulmuş ve oktan ölçümleri yapılmıştır. Oktan hesaplamaları sırasında ASTM tarafından sıvı haldeki yakıtlar için belirlenmiş hesaplama metodu kullanılmıştır. Deneysel olarak ölçülen bu oktan sayıları kullanılarak LPG kompozisyonu ve oktan sayısı arasındaki ilişkiyi kuran matematik modeli oluşturulmuştur. Bu model literatürdeki benzer şekilde yapılmış deney sonuçlarıyla test edilerek güvenilirliği ölçülmüştür.

**Anahtar Kelimeler**: LPG, Oktan Sayısı, Sıkıştırılmış Petrol Gazı, CFR Motoru

To My Family

## ACKNOWLEDGEMENTS

First and above all, I would like to express my gratitude to my supervisor Professor Ahmet YOZGATLIGİL for his guidance and endless encouragements and patience during the thesis study and my graduate education.

This research was supported by the funding from Orta Doğu Teknik Üniversitesi Bilimsel Araştırma Projeleri (BAP-03-02-2017-003).

I would like to express my sincere thanks to Professor Ceylan Talu YOZGATLIGİL, my beloved friends Sina SHAFEE, Ramin BARZEGAR, Oğuzhan ÇABUK, Doğacan KARA, Zeynep KÜDEN and Sıdıka ÖZKAYA for their personnel and professional support as well as their invaluable friendship support.

I also would like to appreciate AYGAZ for their support which made possible this research and study. Communication and their support have provided continuous progress on this study.

The last but not least, I would like to express grateful thanks to my parents Berna, Ufuk and my sister Tuğçe for their endless love, support and encouragement for my goals.

## TABLE OF CONTENTS

## LIST OF TABLES

TABLES

## LIST OF FIGURES

FIGURES

## LIST OF ABBREVIATIONS

ABBREVIATIONS

ASTM: American Society for Testing and Materials

CFR: Cooperative Fuel Research Engine

CI: Compression Ignition

CNG: Compressed Natural Gas

CR: Compression Ratio

DoE: Design of Experiment

IDF: Inverse Diffusion Flame

ISO: International Organization for Standardization

LPG: Liquefied Petroleum Gas

MON: Motor Octane Number

NDF: Normal Diffusion Flame

ON: Octane Number

RON: Research Octane Number

SI: Spark Ignition

# CHAPTER 1

# INTRODUCTION

## 1.1. Motivation

Spark ignition engine was developed in 1876 by Otto. In 1892 Diesel invented the compression ignition engine. Since then, internal combustion engines have a significant role in transportation and industrial usage. Now they play a dominant role in the fields of power, propulsion, and energy. However, internal combustion engines suffer from problems like auto-ignition, knock, and emissions. Especially in recent years, emission regulations are much strict than before. Therefore, to overcome these kinds of problems, not only burning characteristics of different fuels but also engine parameters and design factors should be scrutinized.

Nowadays, strict pollution regulations and continuous decrease in crude oil motivate people to research alternative fuels such as LPG (liquefied petroleum gas) and CNG (compressed natural gas), biodiesel, hydrogen. Among these fuels, LPG is the most common alternative fuel for spark-ignition engines due to its lower emissions, ease of maintenance, and transportation. Moreover, the unit cost of LPG usually lower when compared to gas and diesel [1].

Today, over 16 million of 600 million passenger cars powered using LPG in many countries like Poland, Australia, Italy, South Korea, and including Turkey [9]. Despite being an environmentally clean fuel, LPG also has a higher-octane rating than gasoline, which means LPG can withstand higher internal pressures without auto-ignition. That property can be used to achieve higher thermal efficiencies by designing higher compression ratio engines.

However, there are very few studies that examine the octane number of LPG experimentally. Main achievement of this works, determining the octane number of

LPG samples that have different compositions and modeling the octane rating according to experimental data based on various compositions.

### 1.2. Liquefied Petroleum Gas (LPG)

LPG is an alternative fuel for internal combustion engines as well as it can be used for cooking purposes. It is a mixture of variable content; however, it mainly contains propane and butane. Main advantage over natural gas, when it stored in liquid form its energy content is much denser [41]. On the other hand, emission characteristics of the LPG much superior compared to other refined oil products gasoline and diesel [8]. The following table shows the properties of different fuels and LPG.

Table 1.1. *Fuel Properties [41]*

| Fuel Type | *RON* | *Lower Heating Value (MJ/kg)* | *Rel Density* | *Stoic A/F Ratio (Vol basis)* | *Stoic A/F Ratio (Mass basis)* |
|---|---|---|---|---|---|
| LPG (HD5) | 98-103 | 46.33 | 0.51 | 24:1 | 15.7:1 |
| Gasoline | 91-93 | 44.2 | 0.74 | 60:1 | 14.7:1 |
| Diesel | - | 43.25 | 0.83 | - | 14.5:1 |

More than half of the LPG that is produced in all countries is a result of processing natural gas, and the rest mainly comes from crude oil [16]. LPG that produced from natural gas contains propane, butanes, and a small amount of ethane generally. Since crude oil is unlike natural gas contains different substances, if crude oil is the primary source of LPG, butylenes, and propylene can be observed as a by-product of the refining process [8].

Due to its H/C ratio of LPG, which is 2.63:1 LPG offering potentially much better CO2 emissions compared to gasoline and diesel, which have an H/C ratio of 1.8 and 1.85, respectively. Less carbon content produces less carbon-based molecules during the burning process [41]. Another reason why is LPG so popular is the unit price is

much lower than gasoline and diesel in addition to its emission values. Consumers prefer LPG fueled vehicles for cheaper transportation.

### 1.3. Engine Knock

Engine knock is a kind of abnormal combustion, and it can cause severe damages to internal combustion engines. Knock is the name given to the noise which is transmitted through the engine structure when mostly spontaneous ignition of a portion of the end gas-the fuel, air, residual gas, mixture ahead of the propagating flame- occurs [3][7]. Graphic description and knock development are shown in figure 1.1.

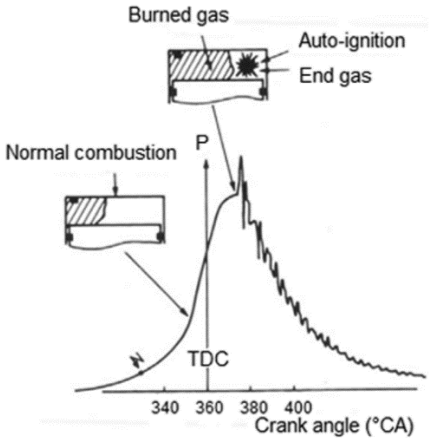


*Figure 1.1.* Knock development in the combustion chamber [3].

Auto-ignition causes rapid heat release, and instantaneous heat release results in high cylinder pressures and pressure fluctuations, which can cause gas motion that reduces boundary layer thickness [4]. Sudden pressure changes and vibrations may result in severe damages to engine components and produce audible noise [6]. In-cylinder pressures in different knock conditions are shown in Figure 1.2.

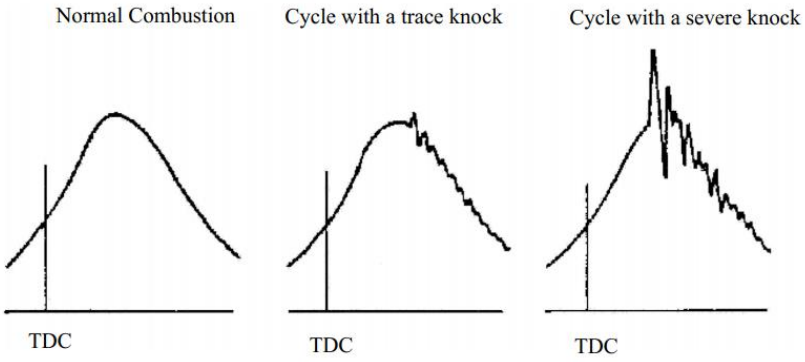


*Figure 1.2.* In-cylinder pressures for different operating conditions [6].

When combustion occurs, high-frequency pressure oscillations can be observed inside the piston. That kind of pressure changes may result in severe engine damage in different ways: piston crown melting, piston ring sticking, cylinder bore scuffing piston ring-land cracking, cylinder head gasket leakage [30][5].

Figure 1.3. shows typical damage resulting from slight and severe knock.

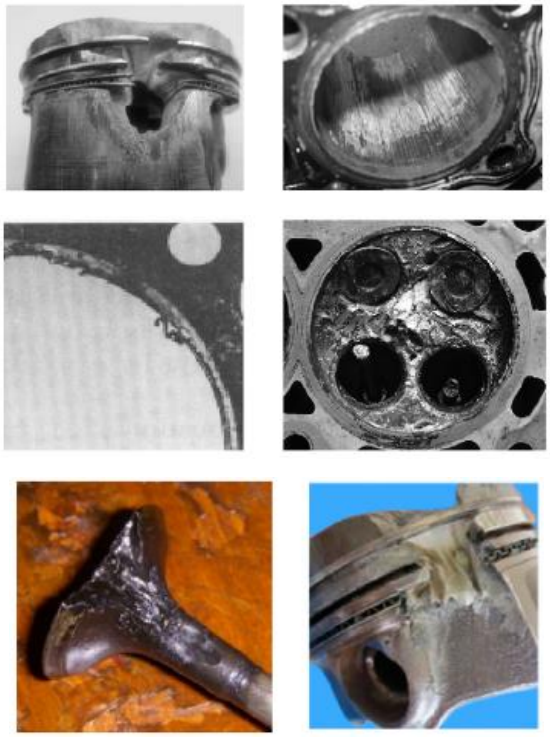

*Figure 1.3.* Typical engine damage due to abnormal combustion [30]

### 1.3.1. Parameters Affecting Knock

Since engine knock is a kind of abnormal combustion, parameters that affect combustion characteristics also have a role in knocking. It can be divided into two major parts: engine parameters and fuel parameters. These topics are discussed below.

#### 1.3.1.1. Fuel Parameters

The ability to resist knock of a fuel depends on its molecular structure and size. In general, more complex molecule chains tend to increase knock resistance due to its molecular bonding. Breaking those bonds requires much more energy, thus knock occurs at higher temperature and pressures [32]. Knock tendencies of the different molecular structures are explained below.

Paraffins,

- In general, an increase in carbon chain length would negatively affect on octane rating due to weaker bond structure.
- A more compact molecular structure because of the shorter carbon chain lengths, has a positive effect on octane rating, which means higher octane numbers.
- Methyl groups ($CH_3$) can be altered the octane number of the fuel, adding a group to molecules in the end or center positions generate non-symmetrical bonding forces which would increase the octane rating of the fuel.

Olefins,

- Double chemical bonds are stronger than single bounded molecular structure, therefore introducing them in the molecule generally increases octane rating and decrease the knock tendency of the fuel. Stronger bonds mean more energy should be added to the system to break molecular chains; therefore, much more heat and pressure should be required inside the cylinder.

Napthenes and aromatics,

- Neptenes introduce significantly higher knocking tendency compared to aromatics
- Since double bonds are much stronger, more than a single, double bond tends to increase the octane rating of the fuel appreciably.

#### 1.3.1.2. Engine Parameters

Engine design changes the combustion inside the cylinder; therefore, every design

Engine design changes the combustion inside the cylinder; therefore, every design parameter affects the knock tendency of the engine. Especially altering inlet and inside cylinder pressure, and the temperature has a significant effect on knock tendency. All these parameters are affected by the combustion chamber design.

The main design parameter is the compression ratio. Compression Ratio (CR) is defined as the ratio of the volume at the cylinder at the bottom dead center to volume when a cylinder at the top dead center. Since CR actually definition of the maximum compression, it has a significant effect on engine knock characteristics. Engines with higher compression ratios tend to suffer from knocking. More pressure and temperature can easily break the bonds of the molecules before controlled combustion occurs.

Other than the CR, almost every parameter that affects the combustion characteristics of the fuel affects knocking tendency. Since modern engines generally designed with forced induction, supercharging, or turbocharging, the engine significantly increases pressure and temperature of the air even before the enters the cylinder; therefore, intercoolers are used to decrease intake temperatures. In some cases, water or water-ethanol mixtures are introduced to achieve higher boost pressures while intake temperature kept lower compared to gasoline.

Moreover, turbulence is another parameter on both combustion and thus knock. A higher tumble swirl inside the cylinder results in a better mixture between air and fuel.

Especially in direct injection engines, valve design, and its turbulence generation have significant importance to reduce engine knock [26].

Spark plug location is also an effect on engine performance and knock like the other engine parameters. Since a spark plug generates a hot temperature spot in the combustion chamber, its location can cause unwanted abnormal combustion and knock. A hot-plug side can have enough energy to start combustion before it generates a spark.

Combustion chamber design may also be one of the parameters that can define engine knock characteristics. Designing a chamber that does not generate a hot spot is the primary goal of a designer.

### 1.4. Octane Number

In order to reflect the knock resistance of the fuels, the octane number definition according to fuel properties is used. Not only a single value, but also two different measurements which are Motor Octane Number (MON) and Research Octane Number (RON) is defined. A higher-octane number indicates that fuel more resistant to autoignition and knock [31]. During testing, various mixtures reference fuels and conditions embedded in experimental design. MON experiments are conducted at higher intake temperatures and higher engine speed. On the other hand, the intake temperature of the RON slightly lower, and engine speed is reduced [30].

Differences between RON and MON testing are given in the table below.

Table 1.2. *RON and MON Test Conditions [30]*

| *Parameter* | *RON* | *MON* |
|---|---|---|
| Intake air temperature | 52°C | 149°C |
| Intake air pressure | atmospheric | atmospheric |
| Coolant temperature | 100°C | 100°C |
| Engine speed | 600rpm | 900rpm |
| Spark timing | 13° bTDC | 14-26° bTDC |
| Compression ratio | 4-18 | 4-18 |

## 1.5. Octane Measurement Techniques

Several octane measurement methods have been developed to create a standard for octane rating. Two of the measurement methods are used to achieve a comparison between fuels, which is one for the research octane number (ASTM D2699), and the other one is for motor octane number (ASTM D2700). As it is discussed in the preceding sections, MON [27] much more suitable for high-performance driving style and in general highway cruising; however, RON [25] is much more suitable for low engine speed city driving. Both methods are defined to use the same single-piston Cooperative Fuel Research (CFR) engine. This test engine is a robust four-stroked, overhead valve engine with an 82.6 mm bore and 114.3 mm stroke.

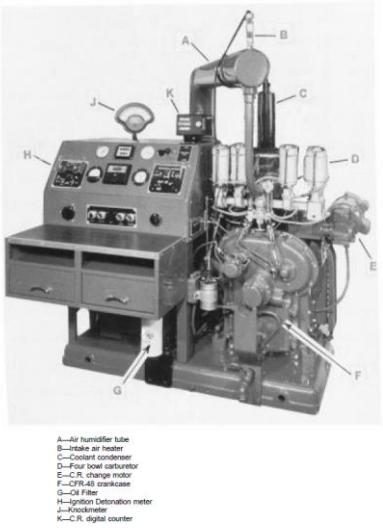


*Figure 1.4.* CFR engine and its components [25]

The compression ratio can be varied while the engine is running from 3 to 30, using a unique mechanism that raises or lowers the cylinder and cylinder head assembly simultaneously relatively to crack the case.

Engine requires two reference fuels, besides, to sample fuel with unknown octane rating. Octane numbers of the reference fuels should be cover the unknown fuel octane number in order to interpolate it according to knock intensity. Test conditions for both RON and MON are summarized in Table 1.1.

Tests should be conducted at maximum knock rating in the defined range. Therefore, the compression ratio, the air-fuel mixture, should be adjusted accordingly. The compression ratio is adjusted to produce a knock of a standardized intensity, as measured with pick-up pressure transducer. The knocking level can be measured with a test fuel that is bracketed by two blends of reference fuels — not more than two octane numbers apart.

Apart from the testing conditions, RON and MON measuring and calculation procedures are identical. However, due to physical conditions on the same test bench, MON of the same fuel is smaller than the RON of the same fuel. The difference between the two values can be defined as fuel sensitivity.

$$Fuel\ sensitivity = RON - MON \tag{1.1}$$

Tests are conducted at wide-open throttle and fixed ignition timing; therefore, they are not very sensitive to predict octane number at general combines performance and city driving. Thus, another definition is called road octane number is developed, which presents the octane number according to general purpose.

$$Road\ ON = a(RON) + b(MON) + c \tag{1.2}$$

a, b, and c coefficients can be calculated depending on experimental results.

To characterization methodology for anti-knock quality, U.S. uses an antiknock index which is the arithmetical average of both RON and MON

$$Antiknock\ index = \frac{RON + MON}{2} \tag{1.3}$$

According to government policies and engine manufactures, octane rating can be defined according to fuels RON and MON rating as it is shown. According to specific needs, a, b, and c coefficients that are in the equation 1.2 can be determined by manufacturers.

### 1.6. Reference Fuels

It is essential to use the nearest higher and lower octane number reference fuels to achieve the best results while predicting the octane number of a fuel. Reference fuels are prepared with a blend of different fuels such as iso-octane, n-heptane, and for the achieve higher octane numbers, tetra-ethyl lead.

#### 1.6.1. Iso-Octane

Iso octane as known as 2,2,4-Trimethylpentane is an organic compound, and its formula can be represented as $(CH_3)_3CCH_2CH(CH_3)_2$. It is used as a reference fuel, which has an octane rating is 100 for both RON and MON [33]. It has very high knock resistant characteristics when compared to regular gasoline; therefore, it can be used as an octane booster additive [35]. The 3D molecular structure of the fuel is shown below.

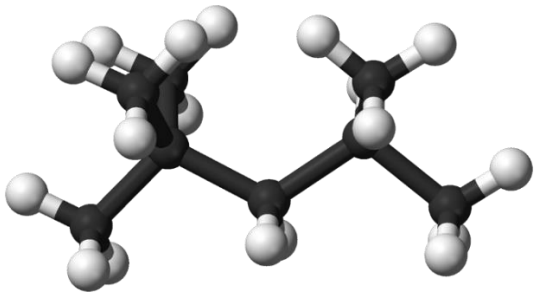

*Figure 1.5.* Molecular Structure of Iso-Octane [36]

Chemical properties of the iso-octane are represented in the table below.

Table 1.3. *Properties of Iso-Octane*

| | |
|---|---|
| Molecular formula | $C_8H_{18}$ |
| Molar mass | 114.2 g/mol |
| Appearance | Transparent |
| Density | 668 kg/m$^3$ |
| Melting point | 166 K |
| Boiling point | 372 K |

### 1.6.2. N-Heptane

Contrary to iso-octane, n-heptane considered as 0 octane rating. Moreover, other octane number fuels between 0 and 100 can be achieved by mixing the iso-octane and n-heptane. The volumetric ratio of those would provide the octane number. For example, 90% iso-octane and 10% n-heptane by volume would result in a fuel with 90 octanes [37].

N-heptane is a straight-chain alkane with a formula $H_3C(CH_2)_5CH_3$, and its molecular structure is given below.

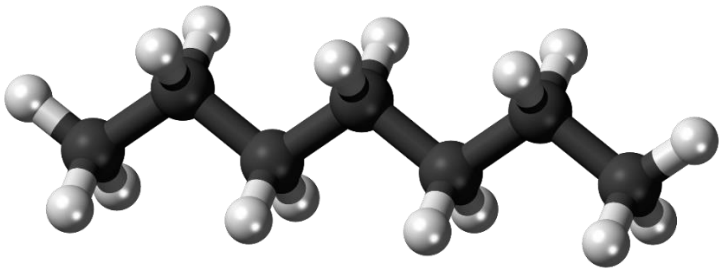

*Figure 1.6.* Molecular Structure of n-Heptane [37]

As it is discussed in the previous section, the leading cause of the lower octane rating is a straight-chain structure. Since energy requirement is much lower for breaking the bonds, it is not so resistant to knock. The chemical properties of the n-heptane are given below.

Table 1.4. *Properties of n-heptane [38]*

| | |
|---|---|
| Molar mass | 100.2 g/mol |
| Appearance | Transparent |
| Density | 648 kg/m$^3$ |
| Melting point | 182.5 K |
| Boiling point | 371.6 K |

### 1.6.3. Tetraethyl Lead

Although iso-octane and n-heptane are defined as fuel, tetraethyl lead (TEL) is only additive and it is one of the most efficient octane agents [40]. It is firstly introduced for aircraft engines to achieve 150 octane fuels. Its chemical formula is $(CH_3CH_2)_4Pb$, and as the formula implies, it contains lead in its structure [39]. The molecular structure is given below. The addition of 0.8 g TEL per liter of gasoline provides an average gain of about ten octane numbers.

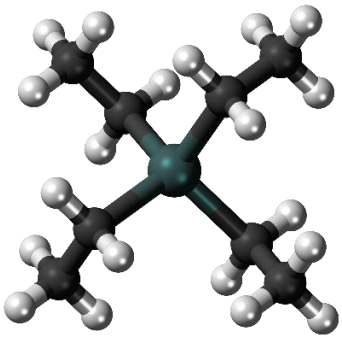

*Figure 1.7.* Molecular Structure of Tetraethyl Lead

Table 1.5. *Physical Properties of Tetraethyl Lead*

| | |
|---|---|
| Molar mass | 323.4 g/mol |
| Appearance | Transparent |
| Density | 1653 kg/m$^3$ |
| Melting point | 137 K |
| Boiling point | 358 K |

### 1.7. Aim of the Study

LPG is a low cost, environmentally friendly, and clean fuel, as is explained in the previous sections. Moreover, its usage of it getting wider each day for automobiles and vehicles due to its low cost and low emission characteristics.

By reference to the literature survey, it is concluded that there are very few studies regarding the effect of LPG impurities and composition on combustion and emissions. Although the octane number is one of the critical factors for internal combustion engines, there is no standard octane testing procedure for gaseous fuels including LPG. Therefore, most of the octane measurement studies are related to liquid fuels and their burning characteristics. Furthermore, as demonstrated in the literature survey, studies for gaseous fuels generally focus on flame characteristics of the fuel.

Unlike the theoretical studies, this research aims to measure the octane number of LPG fuel experimentally by using the CFR engine and determine the effects of LPG composition on knock characteristics.

In this research, a comprehensive set of RON data for mixtures of propane, n-butane, and iso-butane and small amount of ethane and iso-pentane are represented using a method that is consistent with the up to date testing method, which is defined by ASTM for liquid fuels.

The CFR engine modified by Bodur İ. [42] was used to measure octane number of the LPG samples. The fuel system and piston design was revised to work with gaseous and high-octane number fuels.

By using the presented empirical set of data, the octane number of the LPG mathematical modelled according to its mole fractions of compositions. Furthermore, empirical model results compared to other studies and measurements in the literature.

# CHAPTER 2

# LITERATURE SURVEY

## 2.1. Experimental Studies on Octane Measurement of the Fuels

As discussed in Chapter 1, engine knock is a primary limitation on engine thermodynamic efficiency. Even if the increased compression ratio results in higher efficiency and better fuel consumption, it still depends on the engine type and octane rating of the fuel.

High octane fuels allow manufacturers to design engines with a higher compression ratio without suffering from knock phenomena [28]. Due to the importance of the topic, it has been studied in many works, however, mainly for liquid fuels. Although LPG is considered as one of the most influential alternative fuel at present, octane measurement and verification of LPG has received very little attention, and there exist only a few studies about the issue.

Morganti et al. presented an experimental study for measuring research octane and motor octane number of LPG [9]. In this research, ASTM 2699 and ASTM 2700 octane measurements procedure was followed for RON and MON measurements respectively. The study mainly focused on the effects of the primary components of LPG on octane rating, which are propane, propylene, iso-butane, and n-butane. Both RON and MON of twenty-eight various fuel samples that contain mixtures at different ratios and pure components were tested to obtain a mathematical model for the octane number.

According to the research, for predicting octane number of gaseous fuel compositions, regression models for RON and MON were developed and presented as follows [9],

$$RON = 109.4\,X_1 + 100.2X_2 + 93.5X_3 + 100.1X_4 - 5.55X_1X_2 - 4.31X_1X_3 + 2.64X_2X_3 + 4.94X_2X_4 + 59.48X_1X_2^2X_3 + 44.15X_1X_2^2X_4 \quad (2.1)$$

$$MON = 96.3\,X_1 + 83.3X_2 + 89.0X_3 + 96.8X_4 - 2.79X_1X_4 - 3.53X_2X_3 + 6.26X_2X_4 \quad (2.2)$$

Where,

$X_1$: mole fraction of propane in mixture,

$X_2$: mole fraction of propylene in mixture,

$X_3$ mole fraction of n-butane in mixture,

$X_4$: mole fraction of iso-butane in the mixture and the sum of $X_1$, $X_2$, $X_3$, and $X_4$ are supposed to be unity.

Standard error between the predicted and experimented octane numbers were calculated according to the formula below,

$$SE = \sqrt{\sum \frac{(ON_{measured} - ON_{predicted})^2}{N}} \quad (2.3)$$

Moreover, another set of experimental results - that are not included in the regression formula were compared with the regression model in order to test the given formula with different samples.

Silva Jr. et al. investigated the research octane number of ethanol-gasoline surrogates. Ethanol is an alternative fuel that has a higher-octane rating and lower emission characteristics compared to regular gasoline [34]. However, pure ethanol content is not practical at the cold engine start phase due to its low vapor pressure. Therefore, many countries use ethanol as an octane booster. In this research, different proportions of the gasoline and ethanol blends prepared, and their octane numbers experimentally measured on a CFR engine [12].

A pressure transducer was used to measure pressure change inside the combustion chamber. Data collected and 4 kHz – 15 kHz digital bandpass filter was applied to observe pressure oscillations. Figure 2.23 indicates the knock intensity analysis based on cylinder pressure in this paper.

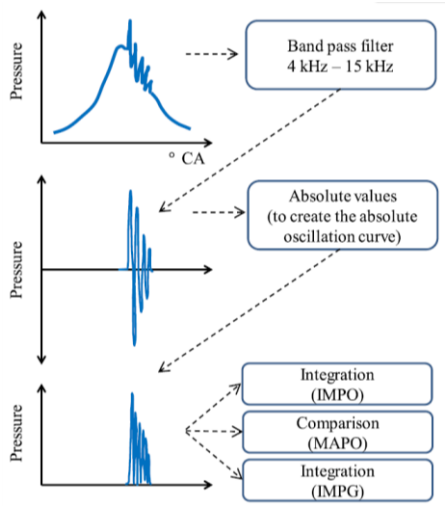


*Figure 2.1.* Knock Intensity Determination Based on In-cylinder Pressure [12]

The determination of the octane rating was performed by using a CFR engine with a variable compression ratio and was conducted according to ASTM 2699 standard. During experiments, the RON procedure of ASTM2699 was followed since it provides more accurate results for ethanol contained fuels. Fuel blends that were used in experiments are given in the table below.

Table 2.1. *Volume Percent of Components in Each Sample [12]*

| Blend | EtOH | *iso*-Octane | *n*-Heptane | Toluene | DIB |
|---|---|---|---|---|---|
| E0 | 0 | 33.3 | 24.4 | 27.8 | 14.4 |
| E10 | 10 | 30.0 | 22.0 | 25.0 | 13.0 |
| E20 | 20 | 26.7 | 19.6 | 22.2 | 11.6 |
| E30 | 30 | 23.3 | 17.1 | 19.4 | 10.1 |
| E50 | 50 | 16.7 | 12.0 | 13.9 | 7.2 |
| E85 | 85 | 5.0 | 3.7 | 4.2 | 2.2 |
| E100 | 100 | 0.0 | 0.0 | 0.0 | 0.0 |

EtOH = Ethanol, DIB = *di-iso*-Butylene.

Experiment results showed that the octane number tends to increase with the increasing ethanol content, as shown in Figure 2.24.

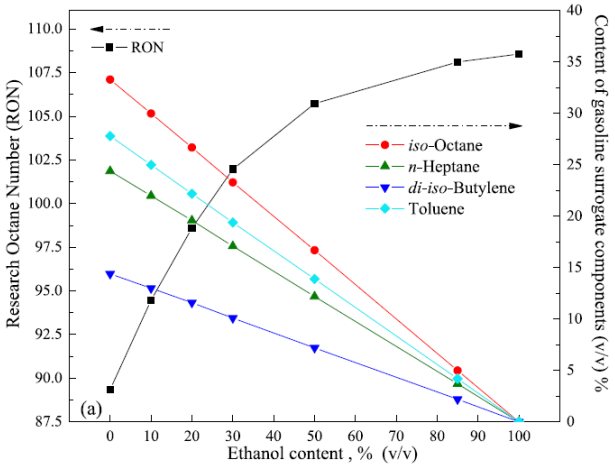


*Figure 2.2.* Measured Research Octane Number for Different Fuel Blends [12]

As Figure 2.2 implies, increasing the ethanol content provides higher octane number fuels (up to 30% (vol.) linear increase in octane number). On the other hand, increasing ethanol content causes problems such as poor cold start performance as low ethanol content fuels can perform better overall in terms of both general-purpose usage and engine performance.

Badra and his colleagues performed another experimental study on the octane number of the various fuels and their ethanol blends. In this research, gasoline surrogates were blended with ethanol, which was one of the main differences in this study from other experimental studies [13].

During the experiments, both the research octane number (RON) and motor octane numbers (MON) are measured using the Advanced Combustion Engine. The study includes five different gasoline surrogates: n-pentane, iso-pentane, 1,2,3,4 trimethyl benzene, cyclopentane, and 1-hexene.

The experimental procedure was modified due to the lower stoichiometric air/fuel ratio of the ethanol when compared to gasoline. This means much more fuel needed to be supplied to the engine when ethanol was the primary fuel. In order to provide fuel at a higher rate, carburetor jets were replaced with bigger ones.

Researchers also modified the air heater due to the high vaporization energy of the ethanol. Since ethanol changes its phase at the temperature of the air-fuel mixture, which is defined by the standard, air-fuel mixture temperature has been kept lower during the experiments. Test results are shown in the following table and figures.

Table 2.2. *RON and MON Measurements for Various Blends [13]*

| | n-Pentane | | *iso*-Pentane | |
|---|---|---|---|---|
| Ethanol vol% | RON | MON | RON | MON |
| 0 | 61.7 | 58.3 | 92.0 | 90.0 |
| 10 | 72.0 | 66.0 | 95.5 | 91.0 |
| 25 | 83.2 | 78.2 | 100.0 | 92.0 |
| 40 | 93.6 | 86.0 | 102.4 | 92.6 |
| 60 | 103.4 | 92.8 | 105.5 | 92.7 |

| 1,2,4-Trimethylbenzene | | Cyclopentane | | 1-Hexene | |
|---|---|---|---|---|---|
| RON | MON | RON | MON | RON | MON |
| 109.5 | 108.0 | 100.0 | 85.6 | 73.6 | 64.5 |
| 107.0 | 102.0 | 101.0 | 85.9 | 81.0 | 68.5 |
| 105.0 | 95.5 | 102.3 | 86.3 | 89.2 | 74.5 |
| 104.0 | 93.5 | 103.3 | 86.6 | 96.5 | 79.5 |
| 105.8 | 91.0 | 104.8 | 87.2 | 101.7 | 84.0 |

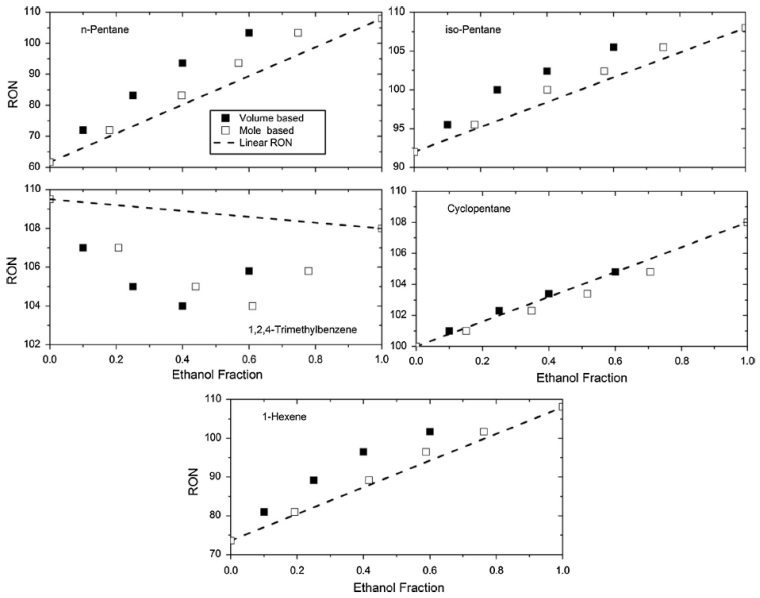


*Figure 2.3.* Measured and calculated RON of Ethanol Blend Fuels [13]

Results indicate that increasing ethanol content in the gasoline surrogates results in a higher RON and MON where n-Pentena, iso-Pentena, Cyclopentane, 1-Hexene are the primary fuel.

### 2.2. Experimental Studies on LPG Emission Characteristics

LPG is not only the economical fuel for the automotive industry but also nature-friendly fuel due to its lower emissions. Moreover, LPG can be considered as the most ecological fossil fuel when it is produced from natural gas because of its low sulfur content, no toxicity, and lack of aromatic hydrocarbons [11].

Comprehensive experimental testing was carried out on a 4-cylinder four-stroke engine by Chitragar et al. [10]. This experimental study aimed to put forward the results of the comparison of three different fuel in terms of emissions, heat release rate, and cylinder pressure. Gasoline, LPG, and pure hydrogen were selected as tested fuels. The main thermophysical properties of these fuels are shown in Table 2.3.

Table 2.3. *Properties of Pure Hydrogen, Gasoline, and LPG [10]*

| Property | Hydrogen | Gasoline | LPG |
|---|---|---|---|
| Density (kg/m$^3$) at 27°C and 1 atm | 0.082 | 730 | 2.26 |
| Lower heating value (MJ/kg) | 120 | 44.8 | 45.7 |
| Higher heating value (MJ/kg) | 141.9 | 48.3 | 50.15 |
| Minimum quenching distance (mm) | 0.64 | 2.0 | 1.73 |
| Minimum ignition energy(mJ) | 0.02 | 0.24 | 0.26 |
| Flammability limits in air (vol%) | 4–75 | 1.3-7.1 | 2.15-9.6 |
| Stoichiometric air-to-fuel ratio (kg/kg) | 34.2 | 14.6 | 15.5 |
| Flame Temp (°C) | 2207 | 2307 | 1960 |
| Auto ignition Temperature (°C) | 585 | 230-480 | 405-450 |
| Octane number | 130 | 87 | 103-105 |
| Flame velocity (m/s) | 2.65-3.25 | 0.3-0.5 | 0.3825 |

As hydrogen fuel does not contain carbon atoms, it does not result in any carbon emissions, which is one of the main issues for other fossil-based fuels. Moreover, it can be extracted from water, all of which make the hydrogen one of the most superior alternative fuels.

The tests in the study by Chitragar et al. [10] was performed at idling speed of 1500 rpm. Since most of the emissions are released during engine idling, i.e., when the

engine stops at traffic lights, or there is slow traffic, the experimental tests on emission performance of fuels are commonly performed at idling speed. Engine specifications of the test engine are given in table 2.4.

Table 2.4. *Engine Specifications [10]*

| Item | Value |
|---|---|
| Engine Make | Maruti Suzuki India Ltd. |
| Engine Type /Fuel | Zen (MPFI), Petrol |
| No. of Cylinders | 4 |
| No. of Strokes | 4 |
| Compression ratio | 9.4:1 |
| Power | 44.5kW @ 6000 rpm, |
| Torque | 78.5Nm @ 4500 rpm |
| Stroke length | 61 mm |
| Bore diameter | 72 mm |
| Capacity | 993 cc |
| Engine Cooling | Water cooled |

To reach the steady-state operation, prior to testing engine was run about 10-15 minutes at idle speed. Exhaust emissions, on the other hand, recorded by a separate AVL gas analyzer.

By recording the pressure data, average cylinder pressures were identified for 100 consecutive cycles depending on the crank angle. The averaged results are depicted in Figure 2.4.

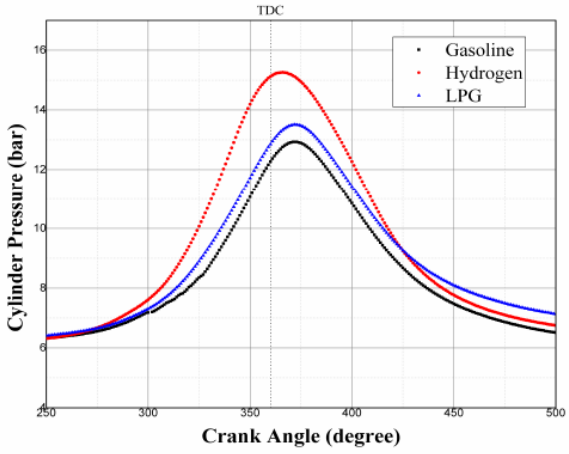


*Figure 2.4.* Cylinder Pressure vs. Crank Angle of Different Types of Fuels [11]

The figure 2.5 implies that when using hydrogen fuel, the maximum cylinder pressure is significantly higher than the other two fuels, the peak occurs in an advanced position, and the pressure curve follows a steeper increasing trend.

Comparing LPG and gasoline also shows that the maximum cylinder pressure of LPG is approximately 0.25 bar higher; however, changes in pressure according to the crank angle are very similar, and peak pressure occurs at a 370-degree crank angle.

Another significant parameter that was measured in this research was the emission rates of fuels. Figure 2.5 indicates the experimental results for CO, HC, and NOx emissions.

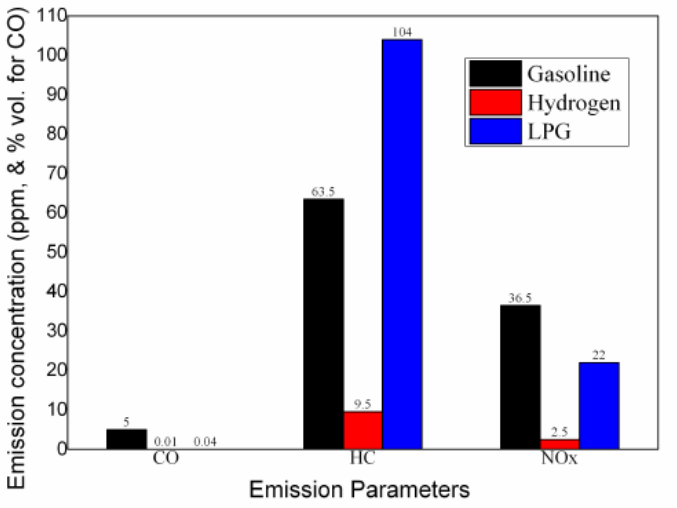


*Figure 2.5.* Exhaust Emissions of Various Types of Fuels

Experimental results also showed that hydrogen provides the lowest CO emissions while gasoline produced 125 times (vol.) more CO emissions than LPG.

HC emissions of LPG were considerably higher than other fuels, and the main reason for it is incomplete combustion [23]. Since hydrogen is much lighter than air, it can diffuse into the air quickly and provide much better entrainment than others. HC emission of the hydrogen is much lower than both gasoline and gasoline as a result of the homogenous mixture and lack of carbon content.

Another performance and emission study when LPG was used as a fuel has been conducted by Çınar et al. [24]. This work mainly concerned a spark-ignited (SI) engine converted to work with LPG. Different cam profiles were manufactured, and performance and emission characteristics were investigated for both gasoline and LPG.

The study also discussed the brake specific fuel consumption (BSFC), which is a crucial parameter for both engine manufacturers and consumers. Engine specifications are given in the table below.

Table 2.5.*Test Engine Specifications [24]*

| Engine model | Four stroke, spark ignition |
|---|---|
| Cylinder number | 1 |
| Swept volume [$cm^3$] | 338 |
| Bore & Stroke [mm] | 82 × 64 |
| Compression ratio | 8.5:1 |
| Maximum engine speed [rpm] | 3800 |
| Valve system | OHC |
| Fuel | Dual fuel (Gasoline and LPG) |
| Valve lift [mm] | 7 (Std valve lift) 8 (high valve lift) |
| Cooling system | Air cooled |
| Maximum brake power [kW at 3800 rpm] | 8.1 |
| Maximum brake torque [N m at 2600 rpm] | 23.7 |

In this research, engine speed and load were adjusted continuously by using a dynamometer while other engine parameters such as air intake temperature and fuel amount were controlled by a computer. Exhaust gas was directed to a gas analyzer through exhaust piping. Moreover, a thermocouple was mounted on the exhaust piping to measure exhaust gas temperature (EGT), which is an essential parameter on emissions [15]. Increasing EGT may result in increased NOx emissions due to the reaction of nitrogen and oxygen at higher temperatures. Figure 2.7 shows the schematic test set up.

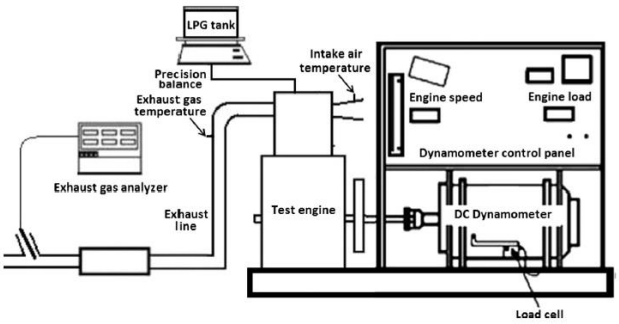


*Figure 2.6.* Schematic Test Set-Up [24]

For these experiments, different cam profiles were manufactured in order to obtain its effects on both liquid and gaseous fuels. Cam profiles are given in Figure 2.8.

*Figure 2.7.* Manufactured Cam Profiles [24]

Brake torque as a function of engine speed was compared using different cam profiles and fuels. The results are depicted in Figure 2.9.

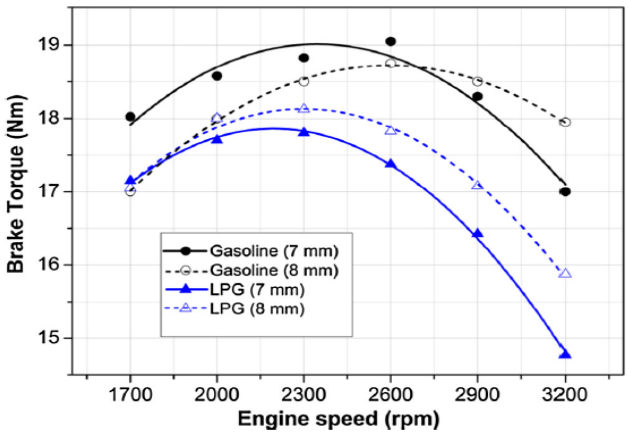


*Figure 2.8.* Brake Torque of LPG and Gasoline for Different Valve Profiles [24]

As the figure indicates, except very low engine speeds, the test engine is producing higher torque with gasoline. Especially at higher engine speeds, the difference is more considerable due to the lower volumetric efficiency of gaseous fuels. Moreover, the higher cam profile resulted in lower torque at especially low-mid RPMs. The same was not applicable for LPG, at each engine speed higher cam profile performs much better results. Secondly, to observe emission characteristics, HC, CO, NOx, and $CO_2$ emissions were measured by a gas analyzer. The following figures show the emission measurements.

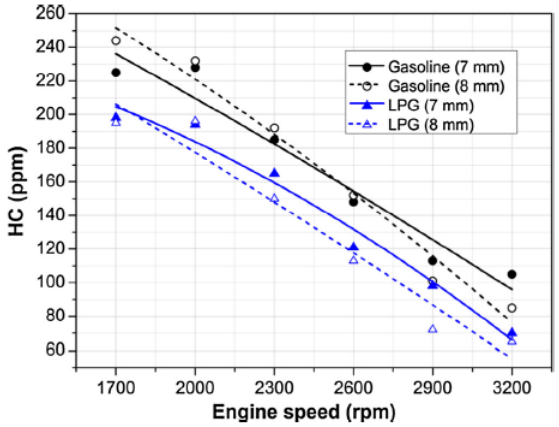


Figure 2.9. HC Emissions of LPG and Gasoline for Different Valve Profiles [24]

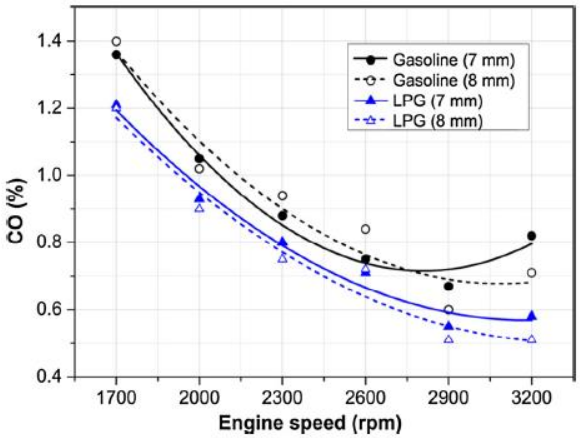


*Figure 2.10.* CO Emission Variation at Different Engine Speeds for Two Different Cam Profiles [24]

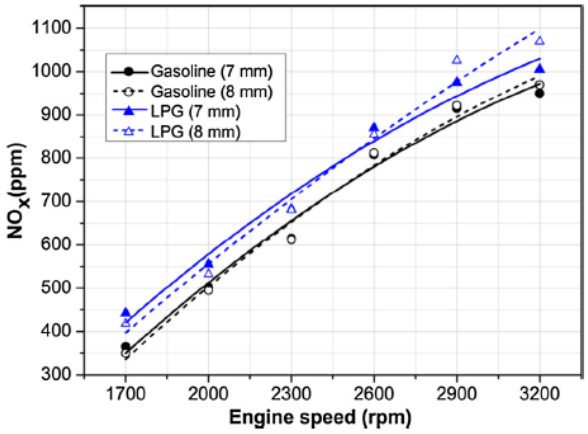


*Figure 2.11.* NOx Emissions of Gasoline and LPG for Different Valve Profiles [24]

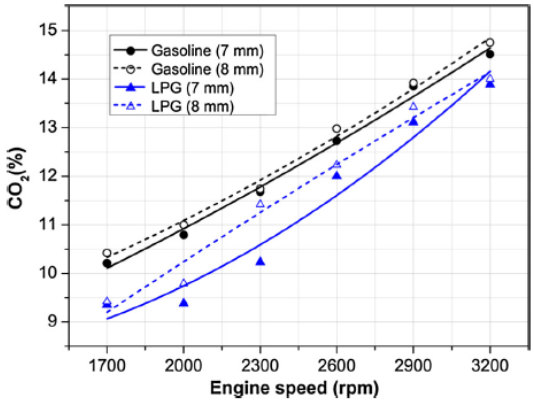


*Figure 2.12.* $CO_2$ Emission Variation at Different Engine Speed for Different Cam Profiles [24]

According to the results, LPG produces significantly lower HC emissions compared to gasoline. For both fuels, HC content in exhaust gas tends to decrease while engine speed increases. Correlation between HC emissions and engine speed seems almost linear even in the case that different fuels are used. Results also indicated that due to the higher combustion temperature of the LPG, NOx emissions are higher than gasoline at each engine speed and cam profile.

Even though LPG has higher NOx emission than gasoline, and it reduces the engine performance, these issues could be resolved in the future by designing a higher compression ratio engine with proper emission reduction systems.

## 2.3. LPG Flame Characteristics

Today many automotive manufacturers are trying alternative fuels due to strict emission and fuel consumption regulations. Among the other feasible options, gaseous fuels are the better options for automotive usage. Despite the fact that hydrogen has the least emissions due to lack of carbon content [21], LPG can also be considered as a more feasible low emission alternative fuel because of its higher-octane number, high calorific value and lower carbon content [11].

LPG flame characteristics is the other parameter that can provide better emissions results. Therefore, there are comprehensive studies on this topic. Especially experimental studies show results with a mixture of different components and different burning characteristics [20].

Swarker and his colleagues [18] investigated the LPG flame characteristics by applying external pulsations generated by a cam mechanism connected to a DC motor. The test was performed at different fuel flow rates. Capturing flame speed was performed with a high-speed digital camera where frame by frame analysis can be possible using image processing techniques.

Experimental setup of the study shown in figure 2.14, which includes a combustor with a 2 mm inner diameter fuel nozzle, which is connected to a circular pipe of diameter 15 mm.

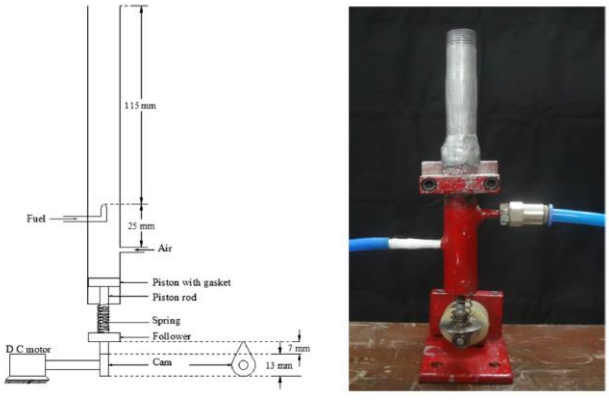


*Figure 2.13.* Test Setup [18]

The piston-cylinder configuration was attached to the burner. That mechanism was located under the combustor and secured with a gasket in case of a leakage. Cam follower mechanism can provide 5 mm displacement; moreover, it is coupled with a DC motor to create external pulsations.

The LPG sample used in the study consisted of approximately 25% propane, 54% butane, and 21% higher hydrocarbon. An air compressor supplied air with a constant 1 bar, which was regulated via an external regulator to achieve premixed composition. In this study, all experiments were conducted at 0-275 rpm pulsation frequencies.

When the experiments were performed at the low fuel flow rate, pulsation speed was relatively high when compared to fuel flow speed, which causes a drastic change in flame flickering. The following figures show the high-speed camera photographs of flames at different times with and without pulsations.

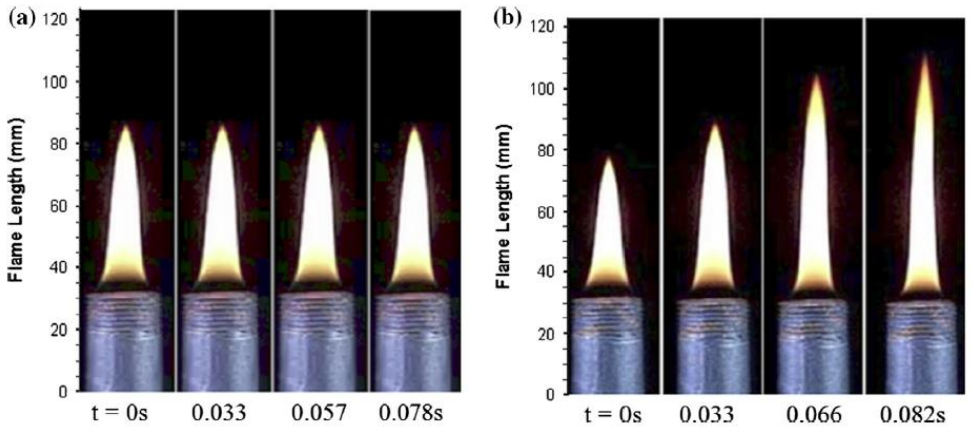


*Figure 2.14.* Images at low fuel flow rate without pulsation (left) and with pulsation at 175 rpm (right) [18]

Another set of experiments was conducted at a high fuel flow rate, which requires much higher fuel velocity. In this case, flickering was observed even the pulsations were not applied to the flame. Figure 2.16 shows the differences in flame oscillations between with and without pulsations at high fuel flow velocity.

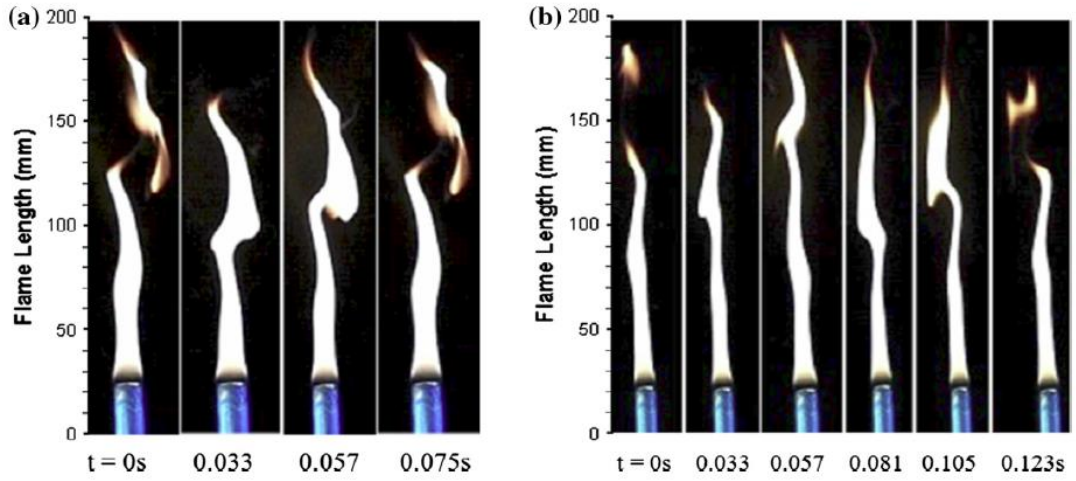


*Figure 2.15.* Diffusion flames at high flow rate; without pulsation (left) and with pulsation at 175 rpm (right) [18]

The authors generated a MATLAB code to process high-speed camera images and measure the flame length. By this method, time-frequency response of the flame at different burning conditions was obtained and using Fast Fourier Transform (FFT); its sinusoidal components have prevailed in order to separate pulsations from base flickering [18].

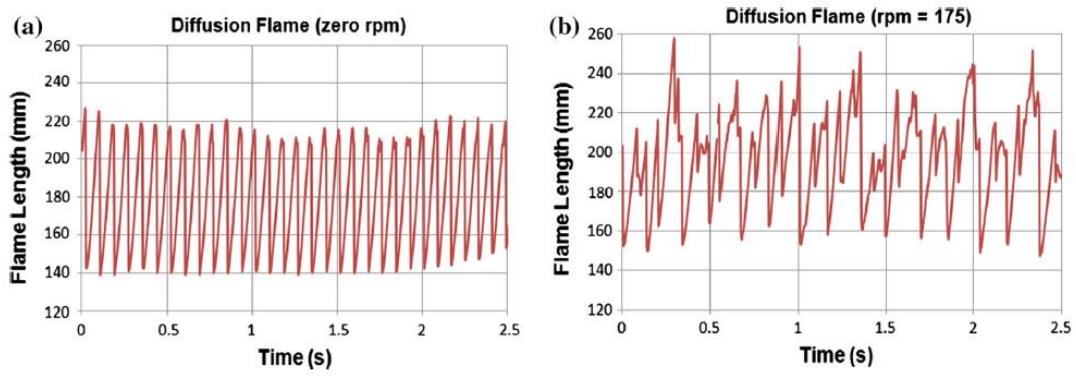


*Figure 2.16.* Flame length variation with time at high fuel flow rate; without pulsation (left) and with pulsation (right) [18]

Patel et al. [17] also investigated IDF characteristics similar to the previous study. Main objective of this work was to reduce soot particle formation when compared to the normal diffusion flame (NDF). IDF is a particular type of non-premixed combustion which defines as an external fuel jet surrounds an internal air jet. IDF

tries to combine both a wide range and stable flame characteristics and low soot emissions [17].

In this study, the coaxial burner was used, which was combined with different types of swirlers. Swirler was placed at the top of the burner in order to create a swirling, turbulent air. However, fuel flow was not disturbed and was supplied through a straight duct.

Schematic representation of the test setup and swirlers are given in figures below.


*Figure 2.17.* Different Swirlers with 8 Vanes [17]

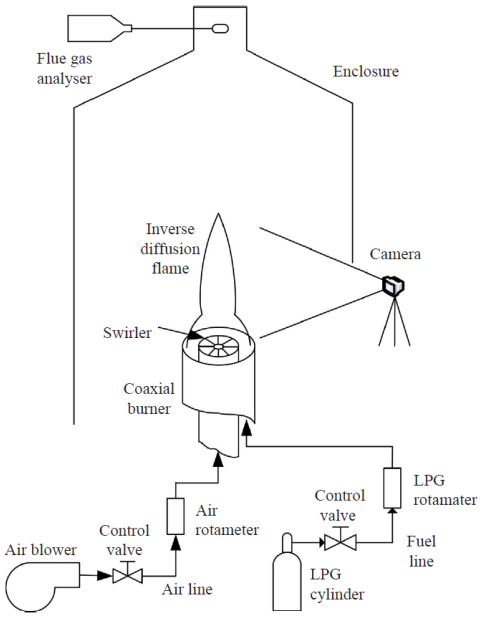


*Figure 2.18.* Schematic Representation of Test Setup [17]

As it is shown in Figure 2.22. an air blower and regulator were used to control airflow and speed in addition to an LPG control valve, which similarly controls the fuel velocity and mass flow.

Experiments conducted at different airspeed and fuel velocity. By disturbing the airflow with swirlers, swirl density was altered before air and fuel mixes. As is represented in Figure 2.8, 3 different swirlers were adopted to the axial combustor.

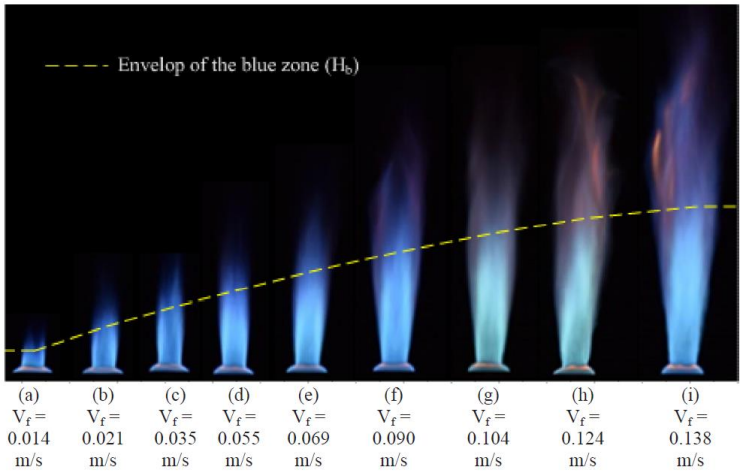


*Figure 2.19.* Flame Images at Increasing Fuel Jet Velocity, $V_a$=18.84 m/s [17]

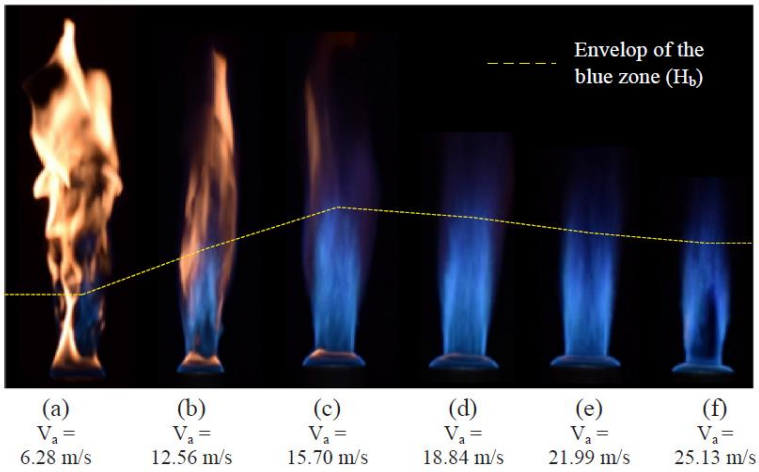


*Figure 2.20.* Flame Images at Increasing Aır Jet Velocity, $V_f$=0.069 m/s

The result shows that an increase in fuel velocity leads to an increase in flame length. On the other hand, increasing air velocity creates a much denser premixed zone, which is identified as a blue flame.

Moreover, overall flame length tends to decrease while increasing the air velocity. Results are very similar to the study, which is performed by Mahesh et al. [20]. The same trend was observed, although the backstep style combustor was used in the research.

As discussed, another set of experiments conducted with different swirlers in addition to different equivalence ratios to obtain both the equivalence ratio and swirl flow effects independently. Figure 2.25 depicts the experimental results of no swirler conditions at different equivalence ratios.

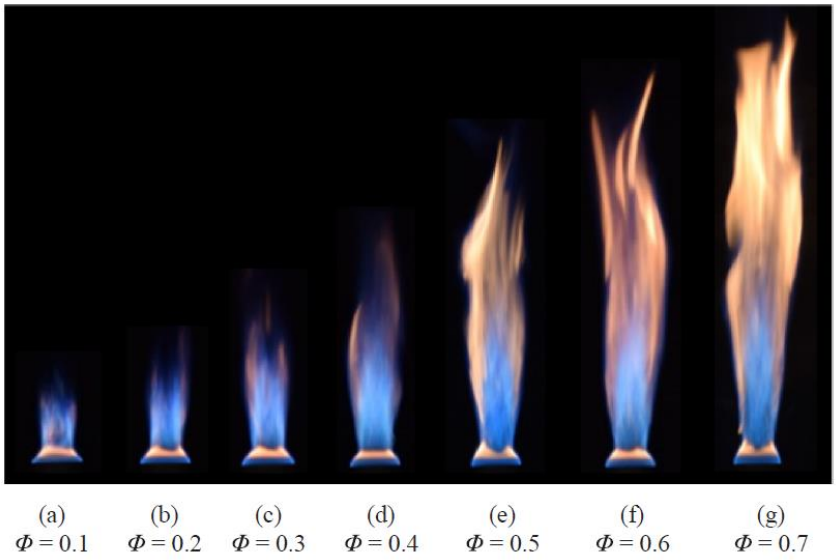


*Figure 2.21.* Effects of Equivalence Ratio on Flame Propagation, $Re_{air}$=9948 [17]

Altering the equivalence ratio has a significant effect on flame propagation, and distinct flame zones can be observed exceptionally high equivalence ratios. The light-yellow illuminance zone is an indication of the non-homogenous mixed air-fuel mixture. Adding more fuel to the system changes the entrainment; thus, two-zone flames occur with relatively high flame length. The same experimental set with

different swirlers provides different types of flames and illuminance zones. The following figures depict the result of the experiments.

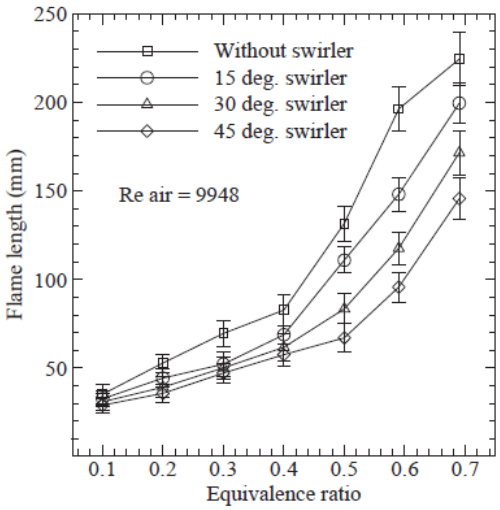


*Figure 2.22.* Effect of Equivalence Ratio on Flame Length [17]

Flame length highly depends on the swirler angle due to the change in velocity components of air on both radial and axial directions. However, the main effect of the swirled airflow provides a much more entrained fuel-air mixture, which is a highly relevant parameter on soot formation. Overall, flame length, on the other hand, is considerably shorter when a high angle swirler is integrated into the burner.

Mahesh et al. investigated the flame length of LPG-air [20]. The goal of their investigation was not only reducing NOx and hydrocarbon emissions but also reducing the soot emission, which was mainly due to non-premixed combustion. Non-premix combustion is widely used in automotive engines, gas turbine engines due to better flame stability, safety, and wide operating limits; however, soot formation is its disadvantage. In the study by Mahesh et al. inverse diffusion flame, which is a type of non-premixed combustion, was investigated [20].

LPG composition consisted of 69% of $C_3H_8$ and 30% of $C_4H_{10}$. In addition to a compressor that provides high-pressure air with a constant rate, silica gel was used to remove moisture from the air.

Imaging was performed on the flame by a high-speed CCD camera. Since it was not possible to measure flame length during experiments, image processing tools were used to analyze photos.

Experiments conducted at different fuel flow velocities and different airflow velocities through constant fuel jet velocities. The results of the experiments were evaluated according to new variable $V_f / V_a$, which expresses the ratio of fuel velocity to airflow velocity. Figure 2.18 shows the flame captures at different air velocities at constant fuel velocity at 0.28 m/s.

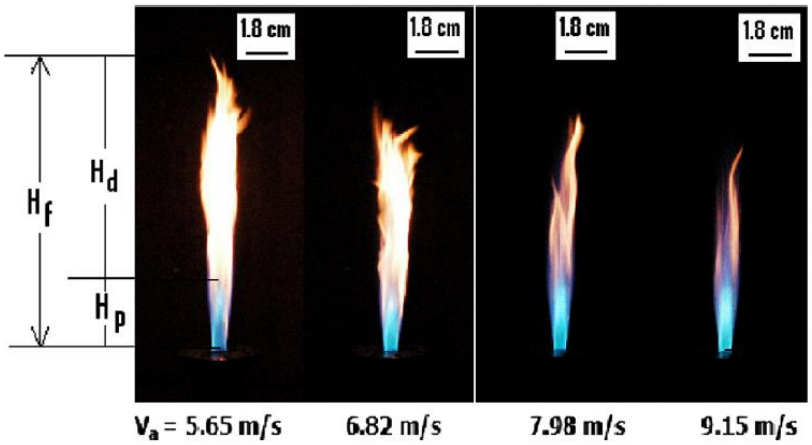


*Figure 2.23.* Flame Lengths at different Va [20]

As Figure 2.18 implies, $H_f$, $H_p$, and $H_d$ defined as total flame length, premixed flame length, and luminous zone, respectively.

Results show that increasing air velocity decreases the total flame length dramatically. Moreover, the blue portion of the flame is 30% longer when compared to slow airspeed. That blue zone is defined as a pre-mixed zone, and a decrease in the premixed zone is an indication of less soot particle as a result of a homogenous mixture of LPG and air [19]. On the other hand, the luminous purple area in the flame is the evidence of an enhanced mixture of LPG and air, which combines with the less total flame length drastically reduces the soot formation due to non-premixed combustion.

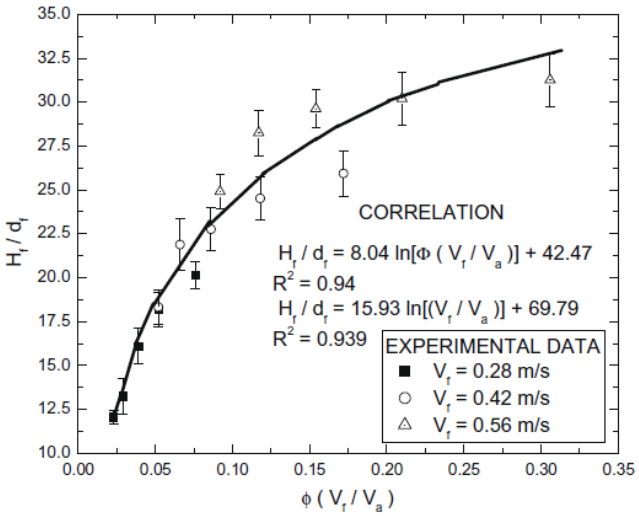


*Figure 2.24.* Correlation for non-dimensional flame length vs. GMR in a backstep burner [20] $10^{-4}$

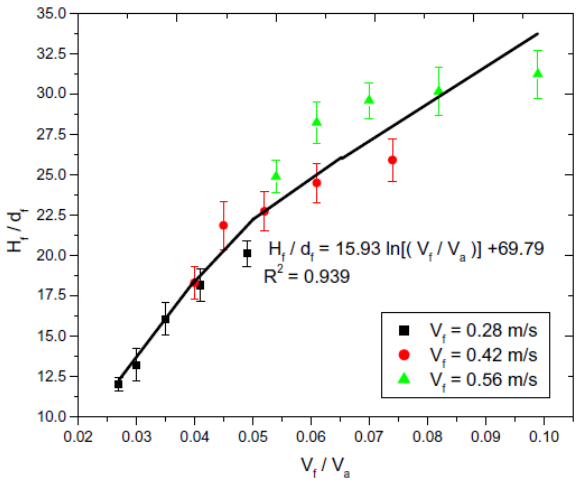


*Figure 2.25.* Correlation for non-dimensional flame length vs. velocity ratio in a backstep burner [20]

Research indicates that soot formation of the non-premixed combustion, which is mainly used in the industry, can be decreased by altering the velocity of the air and the fuel inside the burner. This method creates a pre-mixed zone in the burner and decreases the total flame length. Furthermore, more slander shape flame is the result of the IDF combustion.

# CHAPTER 3

# EXPERIMENTAL SETUP

## 3.1. Cooperative Fuel Research (CFR) Engine

Cooperative Fuel Research (CFR) Engine engines are used many other fuel research applications as well, and not only for octane rating [22]. CFR engine is a four-stroke engine; however, every engine parameter can be adjusted manually, including compression ratio, air-fuel ratio, air intake temperature, ignition timing, and engine speed. Moreover, the engine is equipped with a pressure transducer that measures the inside cylinder pressure [14]. Contrary to the automotive engine, the CFR engine withstands high cylinder pressures, and it is operable under knock condition.

In this study, octane measurement of sample fuels was performed using a modified BASF CFR engine that is located at Middle East Technical University internal combustion engine laboratory.

*Figure 3.1.* Cooperative Fuel Research Engine

Specifications of standard CFR engine that is used in this research are given in Table 3.1.

Table 3.1. *Specifications of a standard BASF CFR engine*

| | |
|---|---|
| Manufacturer | Hermann Ruf Mannheim Elektrotechnische Spezialfabrik |
| Engine Type | 4 stroke, variable compression ratio, naturally aspirated |
| Displacement | 332 cc |
| Bore | 65 mm |
| Stroke | 100 mm |
| Cylinder Head | Removable |
| Piston | Light Alloy, fitted with three sealing rings and one oil scraper ring |
| Crankshaft | Hardened sliding surfaces, double bearing |
| Connecting Rod | Copper-Lead bearings |
| Gudgeon Pin | Hardened |
| Valves and Valve Seats | Hard-faced |
| Low Voltage Ignition | 12 V |
| Lubrication | Forced lubrication of crankshaft, connecting rod, bearing and control wheel; splash lubrication of piston and gudgeon pins |
| Cooling | Water |

On the other hand, an electric motor that is directly connected to flywheel of the CFR engine acts as a starter; furthermore, it is used to ensure that the CFR engine is running at constant engine speed. Desired engine speed can be achieved by altering the pulley diameter of the electric motor. CFR engine is operated at constant 600 rpm and 900 rpm for the RON and MON measurements, respectively. Pulleys with various diameters are shown in Figure 3.2.

*Figure 3.2.* 100 mm pulley for RON (left) and 150 mm pulley for MON (right) measurements

Since MON measurements out of the scope, this research all experiments conducted with 100 mm pulley.

## 3.2. CFR Engine Components

### 3.2.1. Compression Ratio Altering Mechanism

The cylinder head of the CFR engine uniquely designed, and it is connected to the worm gear to adjust the compression ratio. Rotating the compression ratio control lever changes the cylinder height; therefore, the compression ratio. The compression ratio of the standard engine can be adjusted from 4:1 to 12:1. That unique feature is used to achieve desired knock properties with various fuels.

The compression ratio of the engine is controlled with a worm gear fitted to the cylinder support. A hand crank actuates the worm gear, and at every cylinder height, it can be locked by a clamp lever.

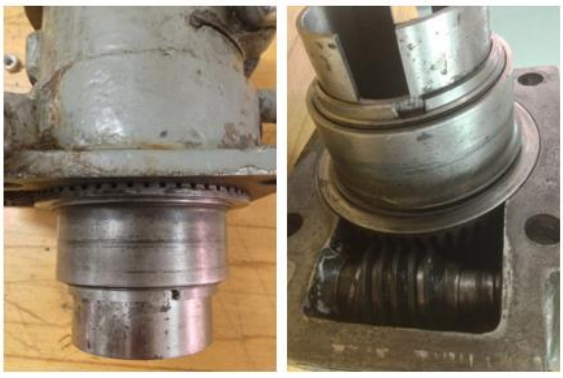

*Figure 3.3.* Compression Ratio Control Mechanism

### 3.2.2. Air Intake Temperature Control Unit

Air intake temperatures of the CFR engine defined by ASTM 2699 standard are 52°C and 149°C for RON and MON measurements, respectively. To achieve specified temperatures, the CFR engine fitted out with a heater, which is located on top of the air intake system. Figure 3.4 depicts the air intake heater system.

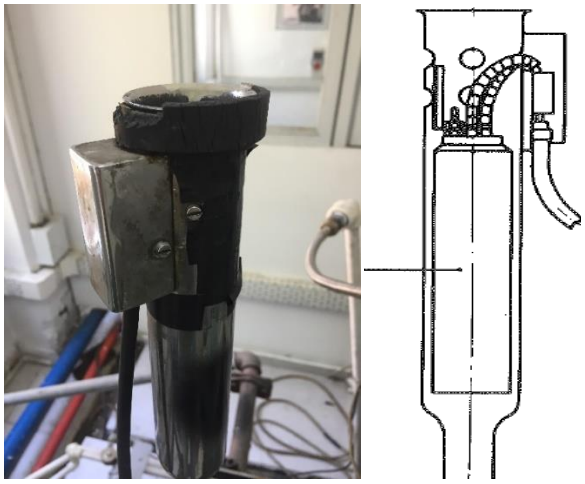

*Figure 3.4.* Air Intake Heater

This heater is controlled automatically by an electronic phase shift controller, and fine adjustment was made using a rheostat, which is mounted to the control unit [8].

### 3.2.3. Pick-Up Transducer

The pick-up is based on the principle of magnetostriction. A rod which is longitudinally magnetized in a constant magnetic field changes its permeance if pressure is applied, changing thereby the magnitude of the magnetic flux. If a coil surrounds the rod, a voltage is produced proportional to the rate of change of pressure [8]. Generated voltage *U* is calculated as the following equation.

$$U = \frac{d\emptyset}{dt} \tag{3.1}$$

Thereby, using proportional correlation, pick-up can be used to measure the pressure inside the cylinder. Voltage data from pick-up can be converted into pressure value or can be used for octane number calculation. Filtering raw data with a proper band-pass filter provides only the time-variant pressure differentials inside the cylinder.

Moreover, the engine is equipped with a control panel, impulses emitted by the pick-up, which are between 200 and 500 millivolts, are passed through an attenuator to the transistorized amplifier. They are differentiated, amplified in the amplifier, and integrated as time average [8]. Since the control panel of the engine is out of use, a pick-up transducer directly connected to data acquisition card and voltage data collected via computer instead.

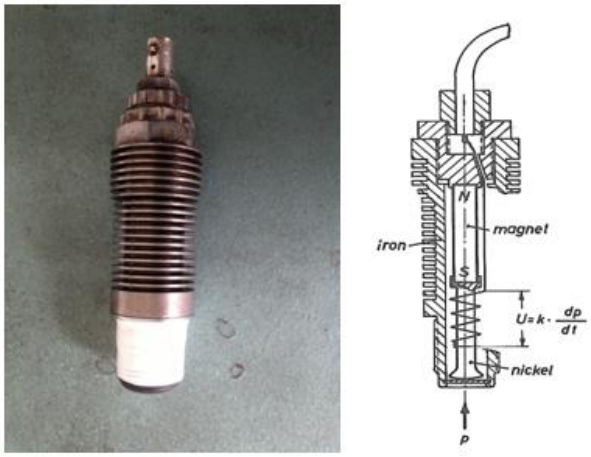


*Figure 3.5.* Detonation Pick-Up

### 3.2.4. Fuel System

Air fuel ratio of the CFR engine controlled by a carburetor, needle below the carburetor allows to adjust air-fuel ratio manually. Also, three fuel trays are connected to the carburetor, and using a fuel selector valve fuel can be supplied from the desired tray. Without draining and refilling, changing the fuel is possible using fuel selection hardware. Moreover, fuel trays contain a glass bowl to maintain float at a constant rate [8].

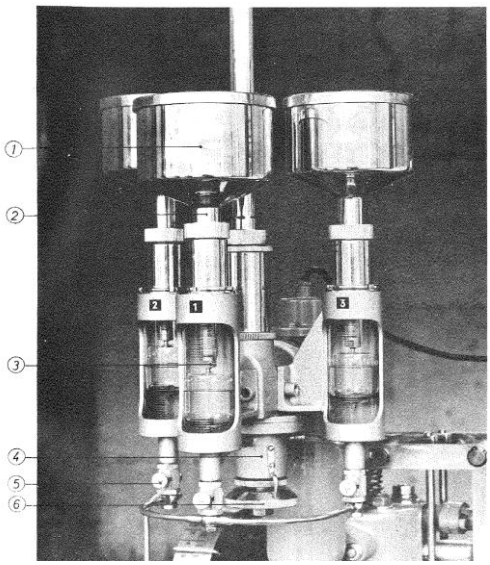


*Figure 3.6.* Fuel Trays of CFR Engine

### 3.3. Engine Modifications and Maintenance

The standard engine is designed to measure the octane number of liquid fuels up to 100 octanes. However, the primary purpose of this research is to measure the octane number of the LPG; therefore, the fuel supply system was modified to operate the engine with gaseous fuels. Moreover, generally, commercial LPG has an octane number above 100, and the engine is not designed to achieve such high-octane numbers. To overcome this problem, a new piston was designed and replaced with the original one.

During this process also damaged parts were reconditioned in order to maintain inside cylinder pressure leakage, proper cooling, and collect data. Reconditioning process includes the head-gasket replacement, cylinder head milling to remove imperfections from the part surface, and slightly changed piston design to achieve higher compression ratios for higher octane number fuels.

All engine modifications performed by Bodur İ. [42] for another study, the same test setup is used to compare measurements and combine the results to perform statistical analysis on the octane number of LPG based on its composition.

### 3.3.1. Piston Modifications

Since LPG has a higher-octane rating than gasoline, for octane measurements, the higher compression ratio was required. In order to achieve such a goal, a new piston was designed by Bodur İ. [42], with an increased gudgeon pin- piston head distance by 2.5 mm.

*Figure 3.7.* Piston design comparison of original (Right) and modified design (left) [42]

Furthermore, two blind holes were drilled on the top surface of the piston to avoid valve and piston head contact at TDC. On the other hand, the diameter of the piston remained the same as the stock size.

*Figure 3.8.* Modified Piston Head [42]

Designed piston drawings and dimensions are given in APPENDIX B.

### 3.3.2. LPG Fuel Feed System

A unique LPG feeding system was not designed for the CFR engine, and standard automobile application implemented to engine by Bodur İ. [42].

### 3.3.3. LPG Tanks

During the experiments LPG samples with various compositions are used as a fuel, instead of refilling a stationary fuel tank, small LPG tanks filled with different compositions were used. These tanks have threaded valves and can easily be connected to the fuel supply line. According to the safety regulations, in case of leakage of fuel, tanks are placed far away from the test engine and equipment room, inside a well-ventilated area.

*Figure 3.9.* LPG Tank

### 3.3.4. LPG Vaporizer

LPG transported and stored as a liquid under pressure. However, in this setup, it should be converted to the gaseous state since the LPG feed system is able to inject only gaseous fuel to intake manifold. To warm LPG up, the vaporizer was connected to the fuel supply system. Even if it uses the engine coolant in order to heat liquid fuel up since the environment was hot enough to vaporize LPG engine coolant was not necessary all the time. Furthermore, inside the evaporator, an electronic switch prevents leakage.

*Figure 3.10.* LPG Vaporizer

### 3.3.5. Air Fuel Ratio Control Valve

The carburetor of the CFR engine has its fuel control needle; however, it is not able to control LPG flow. It can only be used when the engine is running with liquid fuels., an additional LPG fuel control valve was used to adjust the air-fuel ratio while using LPG. It allows regulating LPG flow, thereby air-fuel ratio.

*Figure 3.11.* LPG Fuel Flow Control Valve

### 3.3.6. Data Acquisition System

CFR engine has its own integrated data acquisition instruments. However, that system was out of use. Moreover, an integrated system was not able to collect raw data to obtain knock formation and cylinder pressure.

Up to date data acquisition system with an analog data acquisition card and computer integrated to existing CFR engine. However, the calculation methodology was not changed, and the same procedure was followed as it is stated in the standard.

Data acquisition card provided by National Instruments, which has 16 analog and 32 digital input channels. Since data only collected from detonation pick up, only one analog input channel was used during experiments.

*Figure 3.12.* Data Acquisition Card

### 3.3.7. Engine Maintenance

Prior to test execution, the general maintenance procedure for the CFR engine was followed. Engine oil, coolant, and spark plug were replaced. The cooling system, ignition system, fuel trays, carburetor are checked according to the maintenance guide before starting experiments. Also, to ensure there is no leakage from piston rings and gaskets, compression test was performed. In this test, the spark plug was removed and a pressure gage installed instead. Engine was cranked with electric motor, and maximum pressure is read from the gauge at various compression ratio

# CHAPTER 4

# EXPERIMENTAL METHODOLOGY

The experiments were conducted on modified BASF engine as it discussed in Section 3. In addition to mechanical modifications, data acquisition system was also replaced by A/D data acquisition system.

Despite the fact that CFR engine was modified, bracketing methodology for liquid fuels which is provided by ASTM-2699 standard was followed for octane measurements without any changes.

## 4.1. Compositions of LPG Samples

LPG samples that were used in octane testing experiments had been provided by AYGAZ. The samples had a variety of compositions including propane, iso-butane, n-butane and trace amount of olefins.

LPG compositions were arranged to investigate knocking characteristics of LPG fuel in terms of main three components. However, since extracting olefins from the compositions is not easy and costly, instead of pure mixtures that consist of only propane, iso-butane and n-butane, small amount of olefins were introduced in the test samples.

Table 4.1. *Compositions of Test Samples*

| Fuel Composition % (mol/mol) | | | | |
|---|---|---|---|---|
| Ethane | Propane | Iso-Butane | N-Butane | Iso-Pentane |
| 0.15 | 20.29 | 27.49 | 51.83 | 0.24 |
| 0.29 | 30.94 | 21.84 | 46.66 | 0.23 |
| 0.42 | 37.99 | 3.02 | 58.35 | 0.12 |
| 0.66 | 22.96 | 26.54 | 35.01 | 0.71 |
| 0.21 | 22.52 | 24.31 | 52.65 | 0.25 |
| 0.57 | 22.63 | 26.77 | 33.09 | 0.74 |
| 0.12 | 18.3 | 31.76 | 49.57 | 0.24 |
| 0.17 | 18.05 | 25.84 | 55.62 | 0.26 |
| 0.27 | 16.21 | 10.07 | 67.37 | 0.59 |
| 0.14 | 15 | 1.11 | 83.65 | 0.37 |
| 0.2 | 22.92 | 1.09 | 75.44 | 0.34 |
| 0.2 | 24.2 | 1.08 | 74.18 | 0.33 |
| 0.06 | 14.5 | 1.05 | 73.32 | 0.368 |
| 0.07 | 16.3 | 1 | 71.87 | 0.339 |

Preparation stage consist of mixing, waiting and composition check tests. In order to assure homogenous gas mixture, samples were rested approximately 24 hours after preparation stage. By gas chromatography method their final compositions were checked and labeled. During that procedure EN 1547-2007 regulations were followed. Finally, 2lt samples were shipped to METU Internal Combustion Engine Laboratory for octane measurement experiments.

### 4.2. Reference Fuels and Preparation

Octane measurement test procedure requires reference fuels with a known octane number. Individual octane measurement experiments conduct with two reference fuels and sample fuel then octane number of the sample fuel is calculated by using reference fuel data.

Reference fuels that have octane number between 0-100 were prepared by mixing the iso-octane and n-heptane. Since iso-octane and n-heptane have octane number 100 and 0 respectively, volumetric ratio of their blends provides the octane number of blends. On the other hand, reference fuels that have higher octane number than 100 are prepared by using tetra ethyl lead and iso-octane.

18 different reference fuels were prepared by Tübitak MAM – Marmara Research Center, and before sending to METU, their RON-research octane numbers were verified using a standard CFR engine.


*Figure 4.1.* Reference Fuels

### 4.3. Brief Methodology

ASTM D-2699 standard was built for the octane measurement tests of liquid fuels with a standard CFR engine. However, with the modified engine same procedure applicable for gaseous fuels.

Experimental data collection depends on the raw voltage data collected from pick-up transducer while engine running under knock for two reference fuels with a known octane number and sample fuel. Bracketing method, then provide a calculation of the octane number calculation of the sample fuel.

Both data collection and calculation performed by using a computer code that is prepared in MATLAB. Complete code is given in APPENDIX A**.**

Figure 4.2 represents the general flow chart of the experimental procedure.

In the following sections, both experimental data collection and calculation procedures are explained.

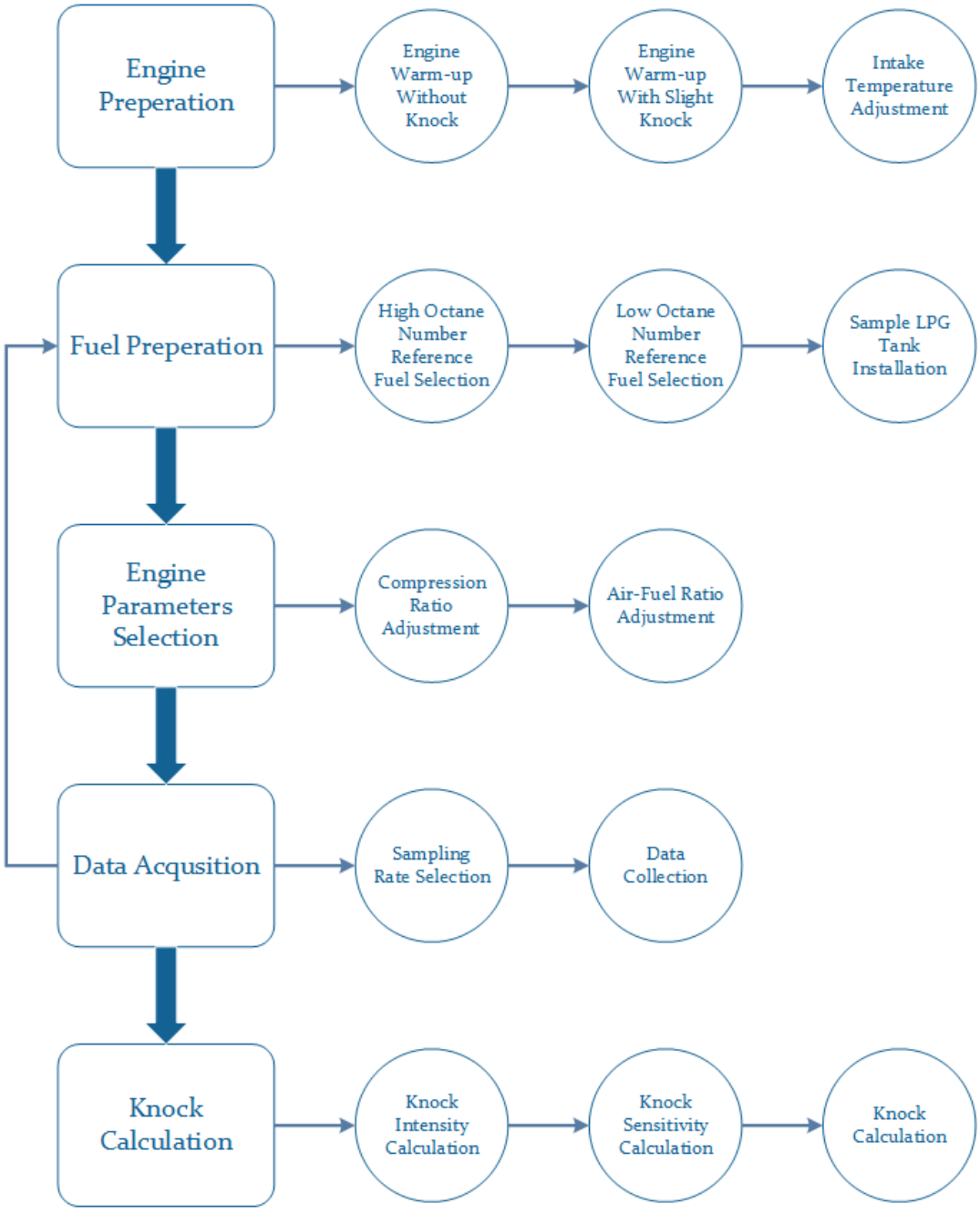


*Figure 4.2.* LPG Octane Measurement Flowchart

### 4.4. Testing Procedure

#### 4.4.1. Engine Preparation

Prior to experiments, engine should be checked for safety and warmed up until it reaches out its operating temperature. Therefore, before the engine started, coolant and oil levels checked in case of any leakage and then, CFR engine started and run before each experiment.

According to octane measurement standard, during preparation phase engine coolant temperature must set to 95ºC, therefore fuel tray of the CFR engine was filled with a regular gasoline and it was turned on. Firstly, compression ratio was adjusted in order to get stable knock free combustion and engine run until coolant temperature reach 80ºC. Then compression ratio was altered to get knock and engine run under slight knock for 15 minutes.

While engine running, air intake heater was also switched on and intake temperature was checked with a laser thermometer.

#### 4.4.2. Fuel Preparation

Octane number measurements requires two different reference fuels with a known octane number. One should be selected such that, octane number should be lower on the other hands, other should have higher octane number than the sample fuel. Therefore, octane number of the sample fuel can be calculated accordingly. Before each test, reference fuels were selected.

Moreover, LPG tank was connected to gaseous fuel feed system of the engine and evaporator switched on to warm up LPG sample.

#### 4.4.3. Engine Parameters Adjustment

When engine coolant and intake temperature reached out to specified conditions, fuel tray of the CFR engine was filled with high-octane reference fuel and detonation pick-

up was connected to data acquisition system to observe voltage data from the pick-up transducer.

While checking the voltage data, firstly air-fuel ratio was adjusted until maximum voltage obtained. Then compression ratio was altered by changing the cylinder head height until voltage read out sits between 0.1-0.2 Volts. When desired value was achieved, compression ratio was set and was not change throughout the rest of the experiment. Then voltage data was collected.

However, even the compassion ratio remained constant, same air-fuel ratio adjustments were performed to get maximum knock readout for lower-octane reference fuel and sample fuel and at the highest knock settings same data collection procedure was followed.

### 4.4.4. Data Collection

Using MATLAB and data acquisition system, sensor readings were collected at 10kHz sample rate which allows to observe pressure changes up to 5kHz cut-off frequency. For a single octane measurement test, data collection procedure was repeated three times for two reference fuels and the sample fuel.

Data acquiring duration was set to 218.16 second for each individual data set which provides 218.160.000 pressure measurements at 10kHz sampling rate. Further analog or digital filtering was not applied to raw data since only maximum inside cylinder pressure is required to calculate octane rating, every data set restored as a separate file.

After data acquisition procedure, engine run for 10 minutes without knock in order to cool it down as it mentioned in the user manual of the CFR engine under shut down procedure section, then it was turned off.

## 4.5. Calculation Procedure

After raw data acquisition, data should be post processed in order to achieve octane number of sample fuel. Bracketing method calculation procedure consists of knock intensity, knock sensitivity and finally octane number calculation.

### 4.5.1. Knock Intensity Calculation

Knock intensity (KI) which is determined by the evolution of the pressure wave following knock onset in a hot spot and highlights the stochastic processes.

KI prediction requires maximum voltage readouts for each engine cycle. Therefore, raw data set have been divided into sub-groups which consist 3030 elements. By averaging the maximum readouts of sub-groups arithmetically, KI was calculated for reference fuels and sample fuel.

Knock intensity calculation matrix and equation are given below.

$$M = \begin{bmatrix} V_{1,1} & \cdots & V_{720,1} \\ \vdots & \ddots & \vdots \\ V_{1,3030} & \cdots & V_{720,3030} \end{bmatrix}$$

$$Knock\ Intensity = \frac{1}{p} \sum_{k=1}^{p=720} M(:,k)_{max} \tag{4.1}$$

Where,

$M$: Raw voltage data matrix

$k$: Column number of the matrix M

$M(:,k)_{max}$: Maximum value of the $k^{th}$ column of matrix $M$

### 4.5.2. Knock Sensitivity

Knock sensitivity is the parameters that represents of a voltage variation per octane number for a single octane measurement data set.

Knock sensitivity can be calculated according to following equation,

$$S = \frac{V_1 - V_2}{N_2 - N_1} \tag{4.2}$$

Where;

$S$: Sensitivity+

$V_1$: Knock intensity of lower octane number reference fuel

$V_2$: Knock intensity of higher-octane number reference fuel

$N_1$: Octane number of lower-octane number reference fuel

$N_2$: Octane number of higher-octane number reference fuel

### 4.5.3. Octane Calculation

Octane number of the sample fuel is calculated by interpolating according to minimum absolute voltage difference.

$$d = \begin{cases} V_2 - V_3, & V_2 - V_3 > V_3 - V_1 \\ V_3 - V_1, & V_3 - V_1 > V_2 - V_3 \end{cases} \tag{4.3}$$

$$N_3 = \begin{cases} N_1 + \dfrac{d}{S}, & V_2 - V_3 > V_3 - V_1 \\ N_2 - \dfrac{d}{S}, & V_3 - V_1 > V_2 - V_3 \end{cases} \tag{4.4}$$

Where;

$V_3$: Knock intensity of sample fuel

$N_3$: Octane number of sample fuel

## 4.6. Control Experiments

Main objective of the control experiments to observe software bugs, engine related problems or calculation mistakes, if there is any and correct them before LPG octane testing.

During control experiments, actual testing procedure was followed in order to check engine condition and calculation methodology. Moreover, other parameters such as ambient conditions, engine temperature, fuels level were kept constant as the actual testing.

In this part, instead of unknown sample fuels, reference fuels with a known octane rating was used as a primary fuel. Since real octane numbers of the fuels are known, they are compared to experimental results and experimental errors are shown in Table

4.2. To check consistency of repeating tests, for each sample fuel experiments performed two times.

Table 4.2. *Results of Control Experiments*

| *RON of Fuel* | *Measured RON* | *Error (%)* | *Measured RON* | *Error (%)* |
|---|---|---|---|---|
| 86 | 85.4 | 0.71 | 85.9 | 0.12 |
| 88 | 87.5 | 0.57 | 88.3 | 0.34 |
| 94 | 94 | 0 | 94.3 | 0.32 |
| 98 | 97.6 | 0.4 | 98 | 0 |

Table 4.2. presents the experimental errors of each measurements, results showing that experimental error is maximum 0.71% for the reference fuel that has 86 octane rating. Moreover, expected error margin is less than 1% for the entire measurement matrix.

# CHAPTER 5

# RESULTS AND DISCUSSION

The RONs for the LPG blends that are given in Table 4.1 are presented, and the mathematical model development method is explained in addition to the comparison of similar studies. All LPG samples were prepared and provided by AYGAZ for this study.

For each constituent, an average RON was determined based on two measurements obtained according to the experimental procedure defined in Chapter 4.

Furthermore, the test matrix extended from 14 to 29 by using measurements from [42], which is a similar study that was performed at the same test setup. The mathematical model developed based on the extended measurements. In general, excellent agreement is obtained between this study and the literature.

## 5.1. LPG Mixtures

LPG compositions that are used in this study does not contain pure substances. Instead, all 29 samples were selected from commercially available due to the high cost and complexity of the preparation and refining process of a particular sample. Hence, these samples are feasible and producible, contrary to pure content. On the other hand, a small amount (up to 0.8%) of ethane and iso-pentane which are the byproducts of refining procedure, were introduced in each sample.

Since samples are produced from natural gas instead of crude oil, they are mainly composed of propane, iso-butane, and n-butane, unlike crude oil, which would introduce propylene additionally.

The test matrix is presented as a ternary plot based on the major components in Figure 5.1 mole fractions are in percentages.

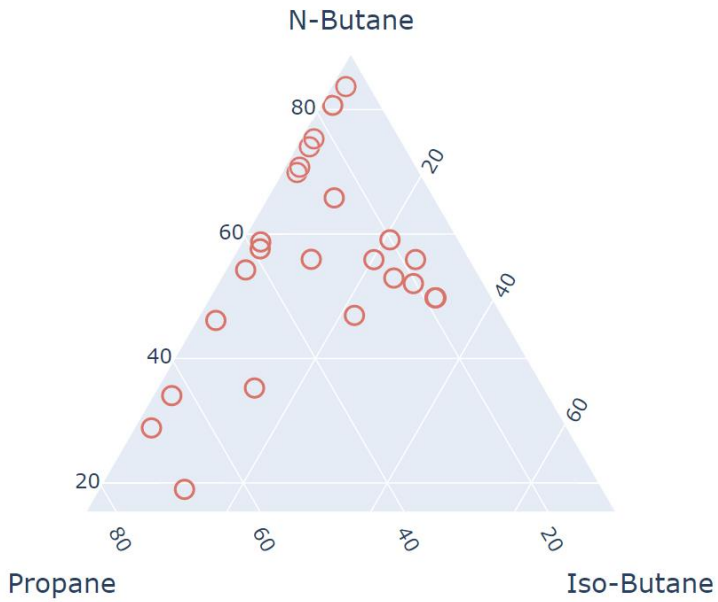


*Figure 5.1.* LPG Sample Compositions Based on Major Components in % (mole/mole)

Figures show that samples include a wide range variety of propane and n-butane, and extended test matrix covers most of the combinations. However, iso-butane content is relatively limited and not exceed 32% in the test matrix, while the others vary from 10 to 80%.

### 5.2. Knock Formation

Pressure change inside the cylinder was obtained from the pick-up transducer that is located on the CFR engine and analyzed for each cycle. When a knock occurs, a sudden pressure rise is expected in the cylinder, similar to the literature. To evaluate knock occurrence in the combustion chamber, the voltage output vs. time graphs are plotted. Voltage output of the pick-up was not converted to pressure since the octane measurement procedure depends on the raw voltage data and conversion procedure requires additional calibration and calculation process.

Inside cylinder pressure variations of consecutive three cycles are given in Figure 5.2.

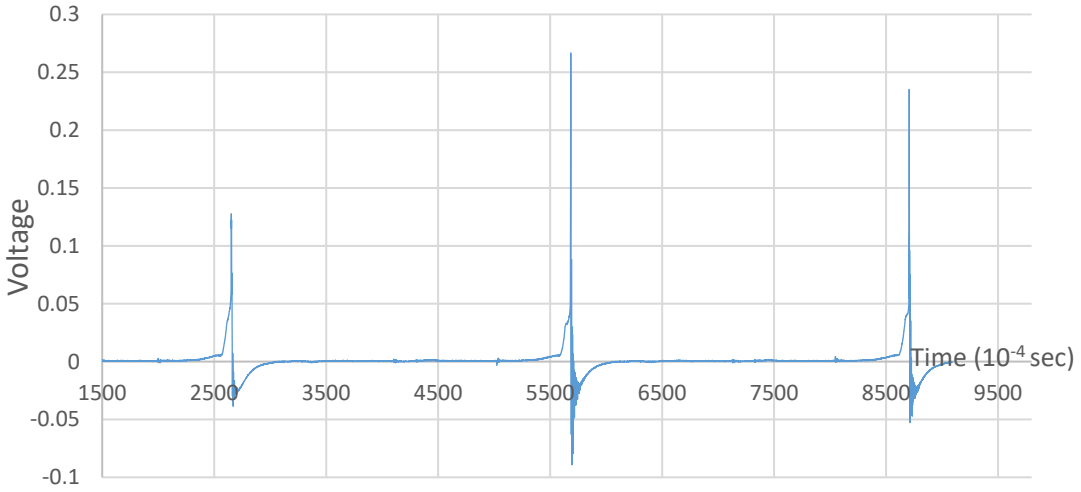


*Figure 5.2.* In Cylinder Pressure Time Variation of Consecutive Cycles

Single-cycle observations provide similar results to the literature, and pressure change in time graph provides good agreement. High-frequency pressure oscillations occur due to knock, and it takes approximately ten milliseconds to reach the equilibrium condition.

Single-cycle pressure observations presented in Figure 5.3.

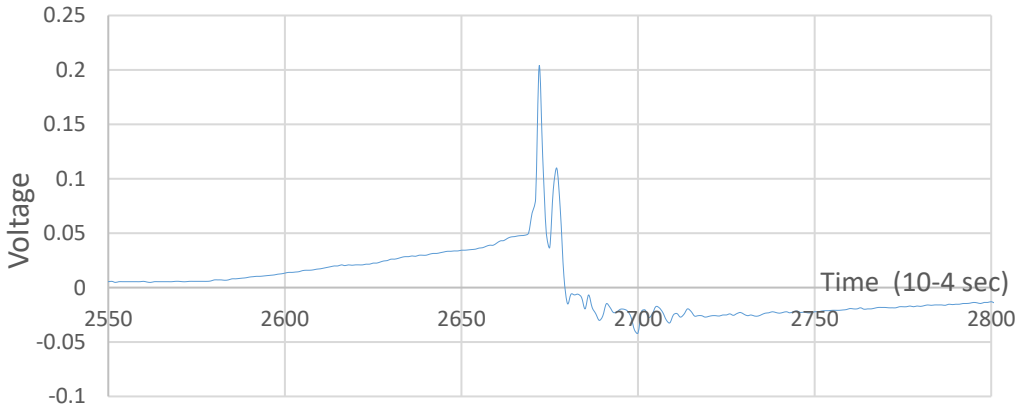


*Figure 5.3.* Inside Cylinder Pressure vs. Time Plot of Single Cycle

### 5.3. LPG Octane Testing Results

Octane number measurements of LPG samples that consist of various compositions were performed and reported for the first time. According to the modified testing procedure for the gaseous fuel, measurements were performed two times at different

times for each sample to eliminate any environmental or experimental uncertainties. The average of the two measurements was considered and used to develop the mathematical model. Compositions and the experimentally determined octane numbers results regarding fuel compositions are given in Table 5.1.

Table 5.1. *Mole Fractions % (mol/mol) and Research Octane Numbers of Test Samples*

| Fuel Composition % (mol/mol) | | | | | RON |
|---|---|---|---|---|---|
| Ethane | Propane | Iso-Butane | N-Butane | Iso-Pentane | |
| 0.15 | 20.29 | 27.49 | 51.83 | 0.24 | 99.9 |
| 0.29 | 30.94 | 21.84 | 46.66 | 0.23 | 100.3 |
| 0.42 | 37.99 | 3.02 | 58.35 | 0.12 | 100.9 |
| 0.66 | 22.96 | 26.54 | 35.01 | 0.71 | 101.2 |
| 0.21 | 22.52 | 24.31 | 52.65 | 0.25 | 100.4 |
| 0.57 | 22.63 | 26.77 | 33.09 | 0.74 | 101.2 |
| 0.12 | 18.3 | 31.76 | 49.57 | 0.24 | 100.2 |
| 0.17 | 18.05 | 25.84 | 55.62 | 0.26 | 99.8 |
| 0.27 | 16.21 | 10.07 | 67.37 | 0.59 | 98.2 |
| 0.14 | 15 | 1.11 | 83.65 | 0.37 | 98.5 |
| 0.2 | 22.92 | 1.09 | 75.44 | 0.34 | 99.2 |
| 0.2 | 24.2 | 1.08 | 74.18 | 0.33 | 98.7 |
| 0.06 | 14.5 | 1.05 | 73.32 | 0.368 | 98.4 |
| 0.07 | 16.3 | 1 | 71.87 | 0.339 | 99.2 |

According to experimental results, octane numbers of samples vary between 98 and 102, which is very consistent with the studies in the literature, when compared to regular gasoline, which has 95 to 98 octane depending on ethanol content octane number of the LPG reasonably high. The experimental test matrix and results are extended with an experimental result, which is presented by [42]. Only test samples that have the same significant substances and have different compositions were selected and combined with the results. Therefore, regression analysis was performed using the combined 29 test measurements. Combined test matrix, LPG samples, and octane measurements are presented in Table 5.2 .

Table 5.2. *Combined Test Results*

| Fuel Composition % (mol/mol) | | | | | RON |
|---|---|---|---|---|---|
| Ethane | Propane | Iso-Butane | N-Butane | Iso-Pentane | |
| 0.15 | 20.29 | 27.49 | 51.83 | 0.24 | 99.9 |
| 0.29 | 30.94 | 21.84 | 46.66 | 0.23 | 100.3 |
| 0.42 | 37.99 | 3.02 | 58.35 | 0.12 | 100.9 |
| 0.66 | 22.96 | 26.54 | 35.01 | 0.71 | 101.2 |
| 0.21 | 22.52 | 24.31 | 52.65 | 0.25 | 100.4 |
| 0.57 | 22.63 | 26.77 | 33.09 | 0.74 | 101.2 |
| 0.12 | 18.3 | 31.76 | 49.57 | 0.24 | 100.2 |
| 0.17 | 18.05 | 25.84 | 55.62 | 0.26 | 99.8 |
| 0.27 | 16.21 | 10.07 | 67.37 | 0.59 | 98.2 |
| 0.14 | 15 | 1.11 | 83.65 | 0.37 | 98.5 |
| 0.2 | 22.92 | 1.09 | 75.44 | 0.34 | 99.2 |
| 0.2 | 24.2 | 1.08 | 74.18 | 0.33 | 98.7 |
| 0.06 | 14.5 | 1.05 | 73.32 | 0.368 | 98.4 |
| 0.07 | 16.3 | 1 | 71.87 | 0.339 | 99.2 |
| 0.3 | 16.7 | 2 | 78.1 | 0 | 97.7 |
| 0.1 | 19.4 | 20.1 | 57 | 0 | 98.8 |
| 0.1 | 17.9 | 30.7 | 48.1 | 0 | 99.5 |
| 0.4 | 26.5 | 1.9 | 68.5 | 0 | 97 |
| 0.3 | 23.7 | 9.4 | 63.7 | 0 | 98.6 |
| 0.1 | 23 | 19.4 | 53.7 | 0 | 99.7 |
| 0.2 | 26.7 | 2 | 68.1 | 0 | 97.8 |
| 0.3 | 31.6 | 11.1 | 54.2 | 0 | 98.9 |
| 0.4 | 37.5 | 3.4 | 55.6 | 0 | 99.2 |
| 0.4 | 41.3 | 3.1 | 52.6 | 0 | 100.7 |
| 0.4 | 49 | 3 | 44.5 | 0 | 101.6 |
| 0.3 | 48.6 | 13.3 | 33.7 | 0 | 101.6 |
| 0.4 | 60.3 | 2.9 | 32.6 | 0 | 102.9 |
| 0.5 | 65.9 | 2.7 | 27.8 | 0 | 104 |
| 0.3 | 66.3 | 11.9 | 18.3 | 0 | 104.9 |

By combining test results, octane variation further increased in a range from 97 to 105. Moreover, an additional 15 experimental results increase the robustness of the regression model due to increased sample variation.

### 5.4. Effects of Components on Octane Number

To investigate the effects of the mole fraction of individual primary components on a RON, it is assumed that each sample contains only three primary substances. Iso-pentane and ethane ignored due to low mole fraction in the samples. Since mole fractions of the components are correlated to each other and sum of them should equal unity, mole fractions of binary mixtures were normalized while other is assumed constant up to 0.5% tolerance range.

Experimentally determined RONs according to binary mixtures of propane, n-butane, and iso-butane are given in the Figure 5.4, 5.5 and 5.6.

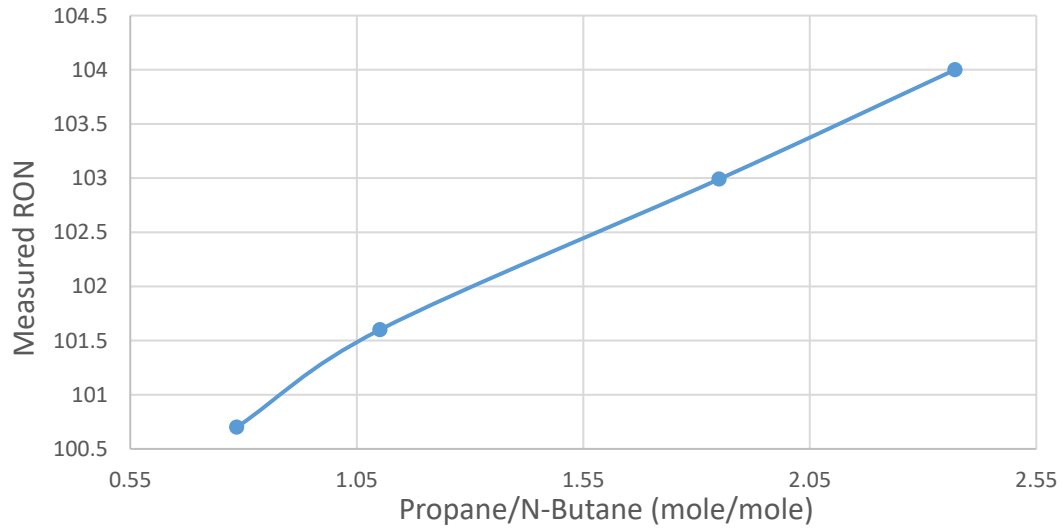


*Figure 5.4.* Binary Effect of Mole Fraction Ratio of Propane/N-Butane on RON at Constant I-Butane Mole Fraction

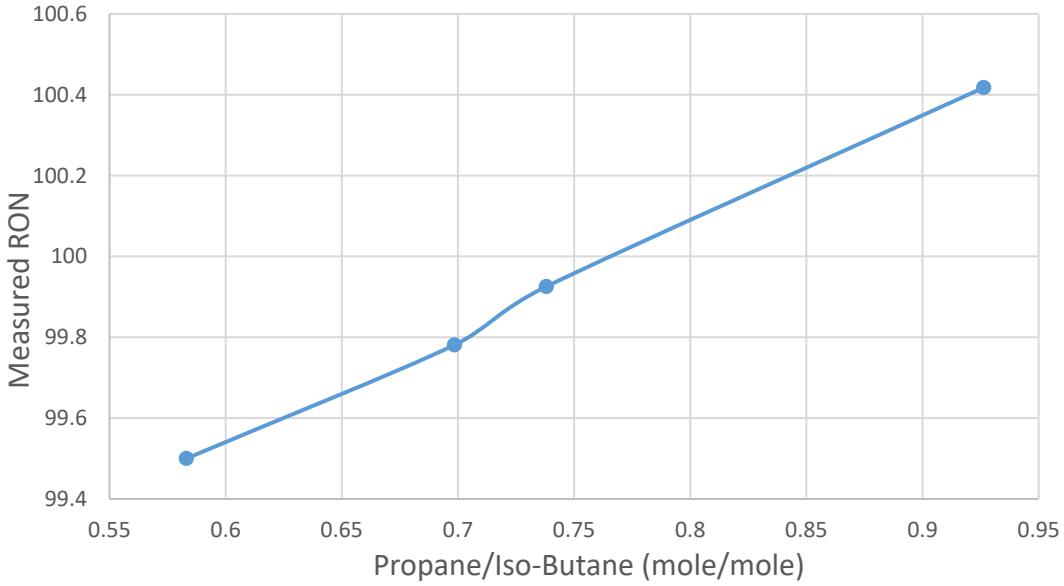


*Figure 5.5.* Binary Effect of Mole Fraction Ratio of Propane/Iso-butane on RON at Constant N-Butane Mole Fraction

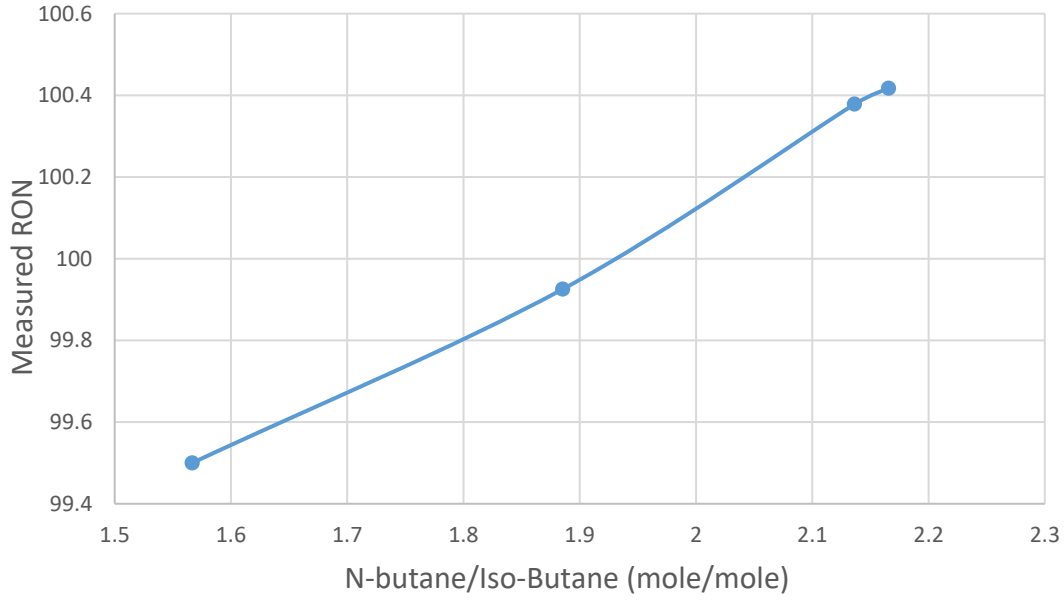


*Figure 5.6.* Binary Effect of Mole Fraction Ratio of N-Butane /Iso-butane on RON at Constant Propane Mole Fraction

By normalizing mole fractions and comparing every combination, dominance of the components is investigated. According to the figures above, RON is linearly dependent on mole fraction of each component. Moreover, propane is the most

dominant parameter of all, and higher-octane number 104 is achieved at a sample that has the highest propane content.

Since RON is linearly correlated for components. A linear regression model is developed to predict octane number of samples.

### 5.5. Statistical Methodology and Regression Model

To reveal the linear relationship between the response variable and explanatory variables, the multiple linear regression model is used. RON is the response (or dependent) variable, and Ethane, Propane, Iso-Butane, N-Butane, and Iso-Pentane are explanatory (or independent) variables. The mathematical form of the model is the following:

$$y_i = \beta_0 + \beta_1 x_{1i} + \cdots + \beta_{13} x_{13i} + \varepsilon_i, i = 1, 2, \cdots, 29 .$$

Where $\varepsilon_i \sim N\left(0, \sigma^2\right)$ are independent, each $x_i$ is independent of $\varepsilon_i$, and $x_i$'s are independent of each other [43]. Using the 29 measurements from the experiment, the variation within the RON variable is explained by the variation in the independent variables. In the modeling, the statistical significance of the parameters is crucial. Here, only Propane, Iso-Butane, and Iso-Pentane variables are statistically significant. Theoretically, N-Butane variable is one of the essential variables to explain the variation in RON, but since it is highly correlated with the other variables, it creates a multicollinearity problem. Hence, the validity of the model cannot be satisfied when N-Butane variable is included in the model. Hence, we did not use it in the model. The model with the three variables explains the 91% of the variation within RON variable. All model assumptions are satisfied. All three variables have a positive effect on RON. When propane increases one unit, RON increases 0.138 unit on the average when other variables stay constant. Similarly, when Iso-Butane increases 1 unit, RON increase 0.073 unit on the average when other variables stay constant. When Iso-Pentane increases 1 unit, RON increase 3.777 unit on the average when other variables stay constant. The correlation between the predicted values and the original RON values is

0.963. The mean squared error (MSE), which is an average squared difference between the observed and estimated values is 0.278.

$$RON = 94.922 - 2.393 * X_1 + 0.147 * X_2 + 0.062 * X_3 + 3.509 * X_4 \qquad (5.1)$$

Where $X_1$, $X_2$, $X_3$, and $X_4$ are the mole fractions of ethane, propane, iso-butane, and iso-pentane in percentages, respectively.

Adjusted R-squared: 0.9207

The regression model was used to predict octane numbers for the mixtures, which is presented in Figure 5.7 . The predicted octane numbers for each mixture correlates very well with the experimental measurements. Furthermore, the MSE=0.278 does not deviate significantly from the corresponding values.

Table 5.3. *Measured and Predicted Octane Numbers According to Fuel Composition*

| Fuel Composition % (mol/mol) | | | | | Measured RON | Predicted RON |
|---|---|---|---|---|---|---|
| Ethane | Propane | Iso-Butane | N-Butane | Iso-Pentane | | |
| 0.15 | 20.29 | 27.49 | 51.83 | 0.24 | 99.9 | 100.1 |
| 0.29 | 30.94 | 21.84 | 46.66 | 0.23 | 100.3 | 100.9 |
| 0.42 | 37.99 | 3.02 | 58.35 | 0.12 | 100.9 | 100.1 |
| 0.66 | 22.96 | 26.54 | 35.01 | 0.71 | 101.2 | 100.9 |
| 0.21 | 22.52 | 24.31 | 52.65 | 0.25 | 100.4 | 100.1 |
| 0.57 | 22.63 | 26.77 | 33.09 | 0.74 | 101.2 | 101.1 |
| 0.12 | 18.3 | 31.76 | 49.57 | 0.24 | 100.2 | 100.1 |
| 0.17 | 18.05 | 25.84 | 55.62 | 0.26 | 99.8 | 99.7 |
| 0.27 | 16.21 | 10.07 | 67.37 | 0.59 | 98.2 | 99.4 |
| 0.14 | 15 | 1.11 | 83.65 | 0.37 | 98.5 | 98.2 |
| 0.2 | 22.92 | 1.09 | 75.44 | 0.34 | 99.2 | 99.1 |
| 0.2 | 24.2 | 1.08 | 74.18 | 0.33 | 98.7 | 99.2 |
| 0.06 | 14.5 | 1.05 | 73.32 | 0.368 | 98.4 | 98.3 |
| 0.07 | 16.3 | 1 | 71.87 | 0.339 | 99.2 | 98.4 |
| 0.3 | 16.7 | 2 | 78.1 | 0 | 97.7 | 96.8 |
| 0.1 | 19.4 | 20.1 | 57 | 0 | 98.8 | 98.8 |

Table 5.3. Continued

| | | | | | | |
|---|---|---|---|---|---|---|
| 0.1 | 17.9 | 30.7 | 48.1 | 0 | 99.5 | 99.2 |
| 0.4 | 26.5 | 1.9 | 68.5 | 0 | 97 | 98.0 |
| 0.3 | 23.7 | 9.4 | 63.7 | 0 | 98.6 | 98.3 |
| 0.1 | 23 | 19.4 | 53.7 | 0 | 99.7 | 99.3 |
| 0.2 | 26.7 | 2 | 68.1 | 0 | 97.8 | 98.5 |
| 0.3 | 31.6 | 11.1 | 54.2 | 0 | 98.9 | 99.5 |
| 0.4 | 37.5 | 3.4 | 55.6 | 0 | 99.2 | 99.7 |
| 0.4 | 41.3 | 3.1 | 52.6 | 0 | 100.7 | 100.2 |
| 0.4 | 49 | 3 | 44.5 | 0 | 101.6 | 101.4 |
| 0.3 | 48.6 | 13.3 | 33.7 | 0 | 101.6 | 102.2 |
| 0.4 | 60.3 | 2.9 | 32.6 | 0 | 102.9 | 103.0 |
| 0.5 | 65.9 | 2.7 | 27.8 | 0 | 104 | 103.6 |
| 0.3 | 66.3 | 11.9 | 18.3 | 0 | 104.9 | 104.7 |

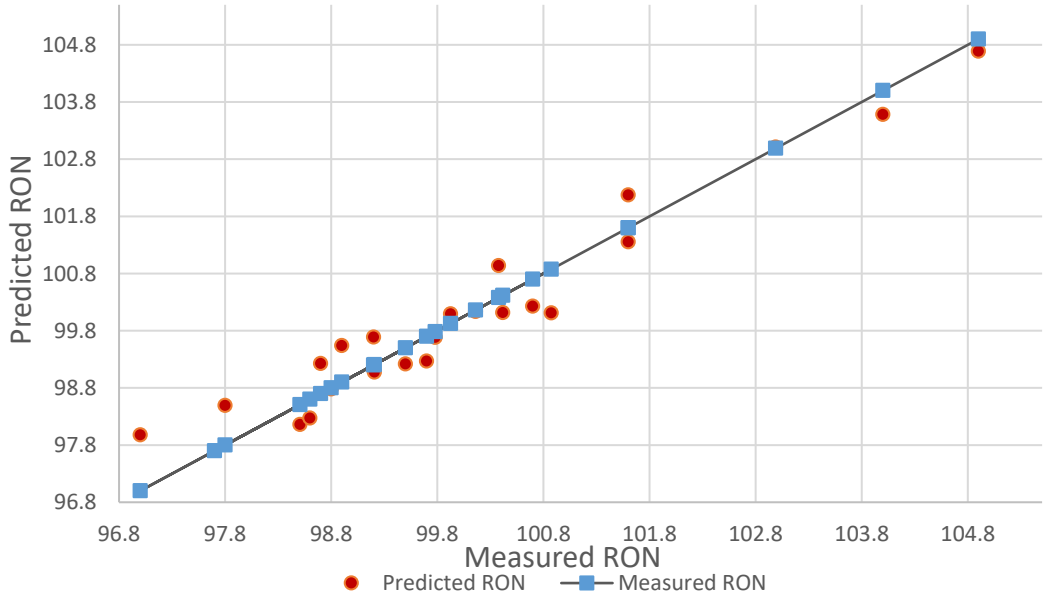


*Figure 5.7.* Measured Octane Number vs. Predicted Octane Number Based on the Regression Model in Equation 5.1

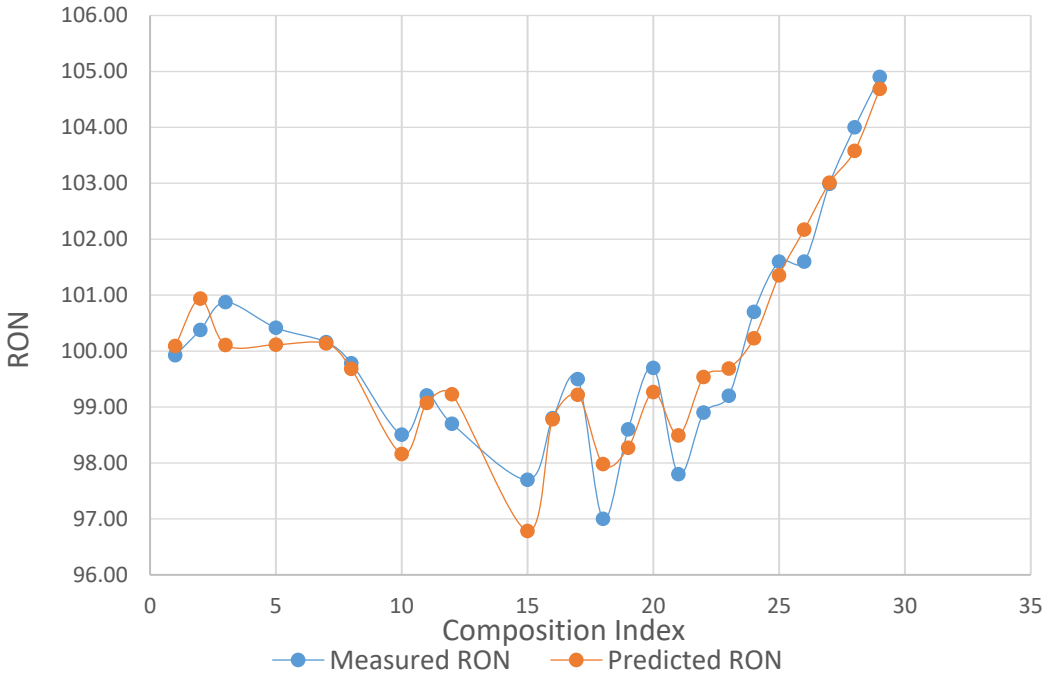


*Figure 5.8.* Measured Octane Number vs. Predicted Octane Number

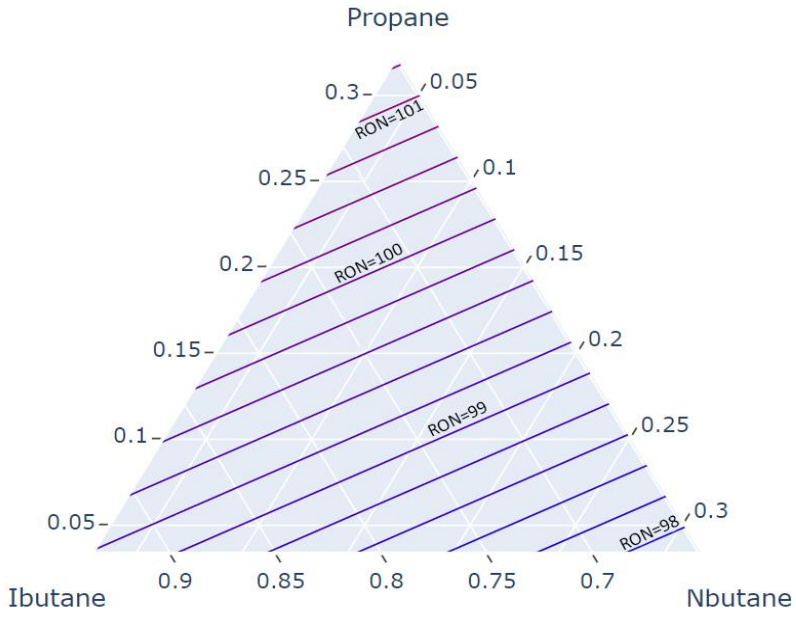


*Figure 5.9.* Constant RON Contour Plot According to Primary Components

## 5.6. Model Comparison

The regression model that was developed by using data obtained from the modified CFR engine is compared to another research. To test the confidence level of the model, empirical measurements performed by [9] is used. Morganti et al. [9] presented 19 different LPG sample compositions which contain three major components and their octane numbers. Test samples are not only including mixtures of propane, n-butane, and iso-butane but also includes pure substances. Design points of the study selected according to the augmented simplex lattice method. Four of these design points located within the interior of simplex and represented ternary mixtures [9]. LPG test sample compositions and measured RON values of [9] compared to RON predictions, according to Equation 5.1 are demonstrated in Table 5.3 .

Table 5.4. *Fuel Compositions and Measured RON [9] vs. Predicted RON According to Developed Regression Model*

| Fuel Composition % (mol/mol) | | | Measured RON | Predicted Ron |
|---|---|---|---|---|
| Propane | Iso-butane | N-Butane | | |
| 100 | 0 | 0 | 109.4 | 109.6 |
| 0 | 0 | 100 | 93.5 | 94.9 |
| 0 | 100 | 0 | 100.1 | 101.1 |
| 50 | 0 | 50 | 100.4 | 102.3 |
| 50 | 50 | 0 | 104.4 | 105.4 |
| 0 | 50 | 50 | 96.8 | 98.0 |
| 66.7 | 16.7 | 16.7 | 104.9 | 105.8 |
| 33.3 | 33.3 | 33.3 | 100.3 | 101.9 |
| 16.7 | 16.7 | 66.7 | 96.6 | 98.4 |
| 16.7 | 66.7 | 16.7 | 100.1 | 101.5 |
| 75 | 0 | 25 | 104.6 | 105.9 |
| 75 | 25 | 0 | 107 | 107.5 |
| 25 | 0 | 75 | 96.7 | 98.6 |
| 25 | 75 | 0 | 102.2 | 103.2 |
| 0 | 25 | 75 | 95.1 | 96.5 |
| 0 | 75 | 25 | 98.4 | 99.6 |
| 41.7 | 16.7 | 41.7 | 100.4 | 102.1 |
| 41.7 | 41.7 | 16.7 | 102.4 | 103.6 |
| 16.7 | 41.7 | 41.7 | 98.4 | 100.0 |

Where $RON_m$ and $RON_p$ are the measured research octane number and predicted research octane number according to (5.1), respectively.

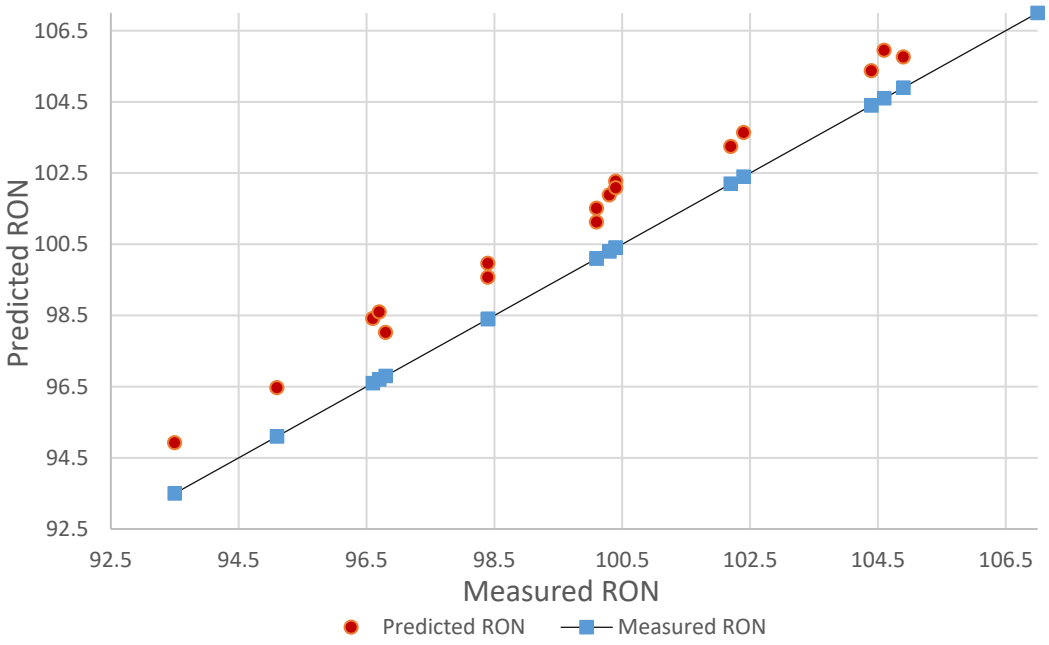


*Figure 5.10.* Measured RON [9] vs. Predicted RON according to Equation 5.1

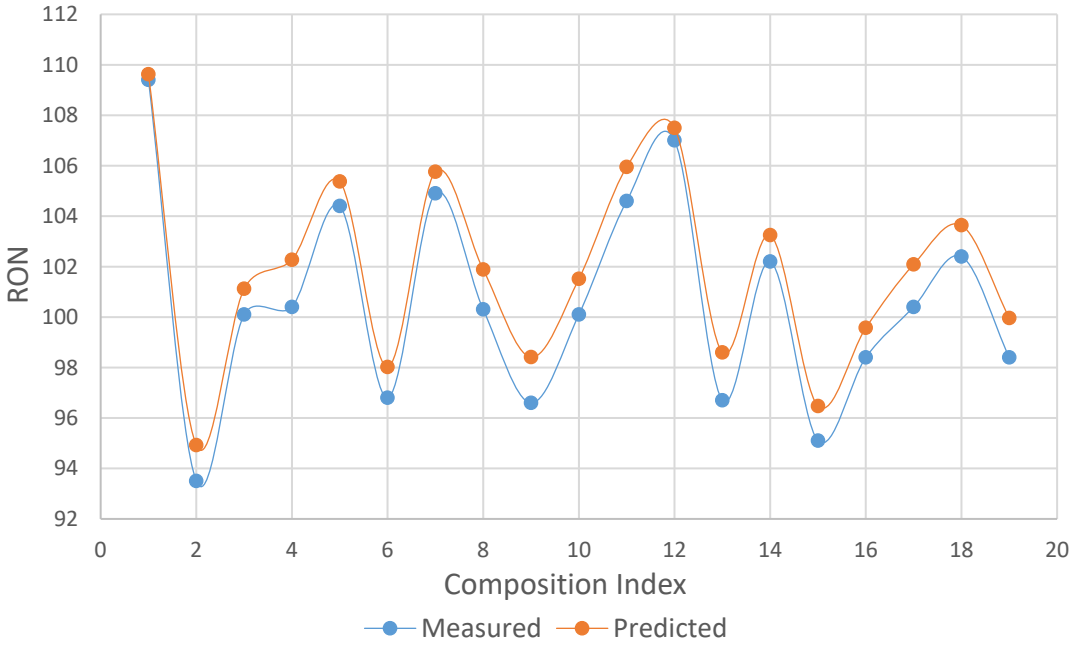


*Figure 5.11.* Measured RON [9] vs. Predicted RON according to Equation 5.1

The developed regression model predicts the RON of the LPG samples that are presented by [9] with a standard error 1.12. However, even though predictions are higher about an octane than the actual measurements, the general trend is very similar and extends through a wide range of compositions, including pure components that are not included in the regression model generation.

Shift in the predicted RON curve mainly occurs due to the impurities of the LPG samples that are used to develop the model. Presented experimentally determined RONs in [9] contain only pure paraffins and their mixtures contrary to presented test matrix in this study. Secondly, CFR engines that were used in both studies are not standard engines. Therefore, mechanical differences such as fuel pressure could be the source of the difference.

### 5.7. Conclusion

This research presented an experimental study of the Research Octane Numbers (RON) of Liquified Petroleum Gas (LPG). A comprehensive set of RON data for the mixtures of primary components of LPG propane, n-butane, iso-butane, and ethane and iso-pentane was presented. To achieve such experimental data, the modified Cooperative Fuel Research (CFR) engine was used. The calculation method and test procedure were not changed; therefore, they are consistent with the current ASTM research test methods for liquid fuels.

Experimental data that is collected during the research combined with the previous study [42], which used the same test setup, in order to achieve a better understanding of the relationship between the fuel composition and octane number.

Both experimentally obtained octane number and knock formation data then compared to data in the literature. Knock formation and pressure variation due to knock occurs as expected and in cylinder pressure reaches an equilibrium state in the expected time period.

The empirical model, which correlates the octane number and LPG composition, was then developed. This model, based on statistical reduction, presents the most straightforward relationship between the constituent species' mole fractions in percentages. The error introduced in the developed model was significantly less than an octane number for most of the cases and reached out to 1.2 at the maximum. Due to the collinearity problem of the main components, n-butane is not included in the mathematical model. Since sum of the mole fractions of the components equal to unity, the combination of other compositions includes the effect of change in n-butane mole fraction.

Since all the LPG test samples are produced by natural gas, they do not contain any propylene. Therefore, it was not included in the model as an independent input. For the LPG compositions that contain a high amount of propylene, the model may not provide sufficient accuracy for the RON estimation.

To test the confidence of the empirical model, experimental RON data of the LPG compositions from literature was used. Although these presented test samples are including pure content, the regression model outputs match very well with the experimentally obtained data. A comparison with the 19 test samples shows that the developed regression model predicts the octane number with an error about an octane number across the range. However, RON trends according to compositions, are very similar.

These observations may be able to LPG producers to fulfill the future LPG fuel quality standards without further testing with expensive and limited test setups. Moreover, it may help to achieve more feasible, commercially available products in terms of cost and performance.

## REFERENCES


[1] D. Maharana and P. A. Soloman, “Flameless Catalytic LPG Combustion and its Optimization Approach,” *Procedia Technol.*, vol. 24, pp. 689–695, 2016.

[2] A. Pillarisetti *et al.*, “Promoting LPG usage during pregnancy: A pilot study in rural Maharashtra, India,” *Environ. Int.*, vol. 127, no. April, pp. 540–549, 2019.

[3] M. S. Lounici, M. A. Benbellil, K. Loubar, D. C. Niculescu, and M. Tazerout, “Knock characterization and development of a new knock indicator for dual-fuel engines,” *Energy*, vol. 141, pp. 2351–2361, 2017.

[4] J. A. Caton, “The interactions between IC engine thermodynamics and knock,” *Energy Convers. Manag.*, vol. 143, pp. 162–172, 2017.

[5] H. Wei, D. Feng, J. Pan, A. Shao, and M. Pan, “Knock characteristics of SI engine fueled with n-butanol in combination with different EGR rate,” *Energy*, vol. 118, pp. 190–196, 2017.

[6] Z. Wang, F. Li, and Y. Wang, “A generalized kinetic model with variable octane number for engine knock prediction,” *Fuel*, vol. 188, pp. 489–499, 2017.

[7] T. Li, T. Yin, and B. Wang, “A phenomenological model of knock intensity in spark-ignition engines,” *Energy Convers. Manag.*, vol. 148, pp. 1233–1247, 2017.

[8] G. Lu and L. Li, “Study on combustion parameters of liquefied petroleum gas engine,” *Energy Procedia*, vol. 12, pp. 897–905, 2011.

[9] K. J. Morganti, T. M. Foong, M. J. Brear, G. Da Silva, Y. Yang, and F. L. Dryer, “The research and motor octane numbers of Liquefied Petroleum Gas (LPG),” *Fuel*, vol. 108, pp. 797–811, 2013.

[10] P. R. Chitragar, K. V. Shivaprasad, V. Nayak, P. Bedar, and G. N. Kumar, “An Experimental Study on Combustion and Emission Analysis of Four Cylinder 4-Stroke Gasoline Engine Using Pure Hydrogen and LPG at Idle Condition,” *Energy Procedia*, vol. 90, no. December 2015, pp. 525–534, 2015.

[11] M. Masi, “Experimental analysis on a spark ignition petrol engine fuelled with LPG (liquefied petroleum gas),” *Energy*, vol. 41, no. 1, pp. 252–260, 2012.

[12] A. da Silva, J. Hauber, L. R. Cancino, and K. Huber, “The research octane numbers of ethanol-containing gasoline surrogates,” *Fuel*, vol. 243, no. August 2018, pp. 306–313, 2019.

[13] J. Badra, A. S. AlRamadan, and S. M. Sarathy, “Optimization of the octane response of gasoline/ethanol blends,” *Appl. Energy*, vol. 203, no. March 2007,

pp. 778–793, 2017.

[14] S. Brusca, A. Galvagno, R. Lanzafame, S. Mauro, and M. Messina, “Fuels with low octane number: water injection as knock control method,” *Heliyon*, vol. 5, no. 2, p. e01259, 2019.

[15] N. K. Miller Jothi, G. Nagarajan, and S. Renganarayanan, “LPG fueled diesel engine using diethyl ether with exhaust gas recirculation,” *Int. J. Therm. Sci.*, vol. 47, no. 4, pp. 450–457, 2008.

[16] B. Liang *et al.*, “LPG characterization and production quantification for oil and gas reservoirs,” *J. Nat. Gas Sci. Eng.*, vol. 2, no. 5, pp. 244–252, 2010.

[17] V. Patel and R. Shah, “Experimental investigation on flame appearance and emission characteristics of LPG inverse diffusion flame with swirl,” *Appl. Therm. Eng.*, vol. 137, no. March, pp. 377–385, 2018.

[18] P. Sawarkar, T. Sundararajan, and K. Srinivasan, “Effects of externally applied pulsations on LPG flames at low and high fuel flow rates,” *Appl. Therm. Eng.*, vol. 111, pp. 1664–1673, 2017.

[19] A. Alharbi, A. R. Masri, and S. S. Ibrahim, “Turbulent premixed flames of CNG, LPG, and H2 propagating past repeated obstacles,” *Exp. Therm. Fluid Sci.*, vol. 56, pp. 2–8, 2014.

[20] S. Mahesh and D. P. Mishra, “Flame structure of LPG-air Inverse Diffusion Flame in a backstep burner,” *Fuel*, vol. 89, no. 8, pp. 2145–2148, 2010.

[21] A. S. Ibrahim, M. A. Abdalwahab, O. S. Abulaban, and S. F. Ahmed, *Investigation of Laminar Flame Speeds of Methane-LPG Air Mixtures*. Elsevier, 2015.

[22] C. Gong, Z. Liu, H. Su, Y. Chen, J. Li, and F. Liu, “Effect of injection strategy on cold start firing, combustion and emissions of a LPG/methanol dual-fuel spark-ignition engine,” *Energy*, vol. 178, pp. 126–133, 2019.

[23] H. Gürbüz, Y. Şöhret, and H. Akçay, “Environmental and enviroeconomic assessment of an LPG fueled SI engine at partial load,” *J. Environ. Manage.*, vol. 241, no. February, pp. 631–636, 2019.

[24] C. Çinar, F. Şahin, Ö. Can, and A. Uyumaz, “A comparison of performance and exhaust emissions with different valve lift profiles between gasoline and LPG fuels in a SI engine,” *Appl. Therm. Eng.*, vol. 107, pp. 1261–1268, 2016.

[25] ASTM Int., “Standard Test Method for Motor Octane Number of Spark-Ignition Engine Fuel 1,” *Annu. B. ASTM Stand.*, vol. i, no. C, pp. 1–56, 2011.

[26] H. Wei, J. Hua, M. Pan, D. Feng, L. Zhou, and J. Pan, “Experimental investigation on knocking combustion characteristics of gasoline compression ignition engine,” *Energy*, vol. 143, pp. 624–633, 2018.

[27] A. I. A. D2700-16, “Standard Test Method for Motor Octane Number of Spark-Ignition Engine Fuel,” *Annu. B. ASTM Stand.*, vol. i, no. C, pp. 1–56, 2016.

[28] G. Shu, J. Pan, and H. Wei, “Analysis of onset and severity of knock in SI engine based on in-cylinder pressure oscillations,” *Appl. Therm. Eng.*, vol. 51, no. 1–2, pp. 1297–1306, 2013.

[29] D. A. Splitter, A. Gilliam, J. Szybist, and J. Ghandhi, “Effects of pre-spark heat release on engine knock limit,” *Proc. Combust. Inst.*, vol. 37, no. 4, pp. 4893–4900, 2019.

[30] Z. Wang, H. Liu, and R. D. Reitz, “Knocking combustion in spark-ignition engines,” *Prog. Energy Combust. Sci.*, vol. 61, pp. 78–112, 2017.

[31] X. Zhen *et al.*, “The engine knock analysis - An overview,” *Appl. Energy*, vol. 92, pp. 628–636, 2012.

[32] Heywood, J.B., “Internal Combustion Engine Fundamentals”, McGraw-Hill International Editions Automotive Technology Series, 2010.

[33] C. L. Barraza-Botet, J. Luecke, B. T. Zigler, and M. S. Wooldridge, “The impact of physicochemical property interactions of iso-octane/ethanol blends on ignition timescales,” *Fuel*, vol. 224, no. March, pp. 401–411, 2018.

[34] H. Xu, F. Liu, S. Sun, S. Meng, and Y. Zhao, “A systematic numerical study of the laminar burning velocity of iso-octane/syngas/air mixtures,” *Chem. Eng. Sci.*, vol. 195, pp. 598–608, 2019.

[35] J. Clayden, *Organic chemistry*, Reprinted. Oxford Univ. Press., 2005.

[36] R. E,George,Totten,Steven,Westbrook, *Fuels and Lubrcants Handbook*, 2003.

[37] A. W. Von Hofmann, “On the Action of Tricholoride of Phosphorus on Salts of the Aromatic Monamines,” *R. Soc. London, 2008*.

[38] W. M. Haynes, *CRC Handbook of Chemistry and Physics*. 2011.

[39] UNEP, “Partnership for Clean Fuels and Vehcles,” *Transport*, 2017.

[40] D. Seyferth, “The Rise and Fall of Tetraethyllead,” *Organometallics*, 2003.

[41] SAE, “Fuel Mixing for Gaseous,” *Tech. Pap, 2002.*

[42] İ. İ. Bodur, “Knock Rating of Gaseous Feuls in a Modified Cooperative Fuel Research (CFR) Engine,” Middle East Technical University, 2015.

[43] Kutner, Nachtsheim, Neter, Wasserman, Applied Linear Regression Models, 4/e, 2004.

# APPENDICES

## A. MATLAB Octane Measurement and Calculation Code

```
clc
clear all
format long
nh=input('Enter Higher Octane Number= ');
nl=input('Enter Lower Octane Number= ');
devices = daq.getDevices
s = daq.createSession('ni')
s.addAnalogInputChannel('Dev1',0,'Voltage')
s.Rate = 10000
s.DurationInSeconds = 218.16
A = s.startForeground();
B = reshape(A,3030,[]);
M= max(B);
C= transpose(M);
D= reshape (C,120,[]);
E = sort(D,'descend');
F= mean2 (E);
```

## B. Experimental Procedure

- Engine coolant circulation turned on.
- Engine coolant level checked.
- Engine switch turned on.
- CFR engine is started.

  At this stage engine running with only its electrical motor. Since fuel is not added there is no combustion inside the cylinder. During this period engine is checked in case of any unwanted damage or any other issue.
- Air heater switch turned on.
- Ignition switch turned on.
- Fuel tank filled with an ordinary gasoline.

  At this stage fuel only used for warm-up period. Engine should be run at normal conditions (without knock) during warm-up period to prevent engine from breaking.
- Carburetor needle adjusted for normal combustion of the engine.
- Engine run at least 15 minutes for warm up without knock.
- CFR engine coolant temperature checked every minute in case of overheating. Testing should be performed at 95ºC coolant temperature. However, coolant only can reach up to 80ºC without any knock.
- After 15 minutes warm up period, engine should be run under slight knock to achieve 95ºC engine coolant temperature.
- CFR engine compression ratio adjusted to get slight knock.
- CFR engine run another 15 minutes under knocking condition and operating coolant temperature 95ºC is reached.
- Drain valve is opened and ordinary gasoline drained away.
- Fuel tank filled with high octane reference fuel.

  If during draining and filling procedure, engine coolant temperature gets lower than 95ºC, engine continue to run under slight knock until it reaches out its operating limit.

- Detonation pick up is connected to data acquisition analog input.
  Since MATLAB code is using only the analog input 1 slot, each time detonation pick-up should be connected to same port. Otherwise, it would cause an error
- National Instrument software has its own oscilloscope view in it. Instead of using secondary oscilloscope for the reading voltage data from detonation pick-up, software is much practical. Sampling rate for the voltage view adjusted to 10kHz that is same with the experiments.
- At this stage, maximum knock should be adjusted between 0.1-0.2 V. To achieve it compression lever loosened and compression ratio of the CFR engine adjusted. Secondly, air flow ratio also adjusted to reach maximum knock. If the voltage reading is higher or lower than specified range, same iteration repeats until the maximum knock reading between 0.1-0.2 V.
- After desired voltage range achieved with the high-octane number fuel, compression ratio remains constant rest of the testing.
- National Instrument (NI) software is closed. Until that point, both MATLAB and NI cannot reach out the data acquisition card. Only one of them should be used. Since there is no need oscilloscope, MATLAB code is loaded to software and NI is closed.

Next steps define the MATLAB code which provide simultaneous data acquisition and post processing. There is no need to separate data collecting and post processing.

- Firstly, MATLAB code requires reference fuel octane number, following code lines takes the octane numbers as an input.

```
clc
clear all
format long
nh=input('Enter Higher Octane Number= ');
nl=input('Enter Lower Octane Number= ');
```

nh and nl defined as octane numbers of reference fuel with high octane number and lower octane number respectively. Used should define both these values in the User Interface.

- Following code section is used to collect data.

```
devices = daq.getDevices
s = daq.createSession('ni')
s.addAnalogInputChannel('Dev1',0,'Voltage')
s.Rate = 10000
s.DurationInSeconds = 218.16
```

First of all, MATLAB defines the connected devices which is data acquisition card in this case and then create a new session to collect data. Session created for the connected device which is defined as “ni”.

Moreover, input channel is defined as an analog input 0 port. If the connection port is different than change should be implemented in the code.

Next two lines defines the data acquisition parameters. s.rate shows the sampling rate of data collection. In this case as it is stated in ASTM D2699 it is 10kHz. S.DurationInSeconds defines the data collection time. In order to achieve desired number of data point it is selected as 218.16 second. Which provide 2.181.600 voltage data.

According to Nyquist rule, cut-off frequency of the signal is half of the sampling rate. Since 10kHz sampling rate is used in this study, 0-5kHz frequency spectrum can be observed. However, further low pass filtering or band pass filtering does not apply to raw data. In calculation methodology, average of the voltage data used as a knock intensity and Butterworth filtering method does not have an effect.

- `A = s.startForeground();`
  command in the next line, starts the data acquisition and writes all data to an array which is called A. In this step MATLAB uses binary coding for mass

raw data contrary to EXCEL. By this method sample files need much less storage in the hard drive and memory. Moreover, EXCEL has a line limitation and it is not possible store raw data file as a single line.

- After high octane reference fuel data collection, a warning is shown on the user interface to change reference fuel with the reference fuel which has a low octane number.

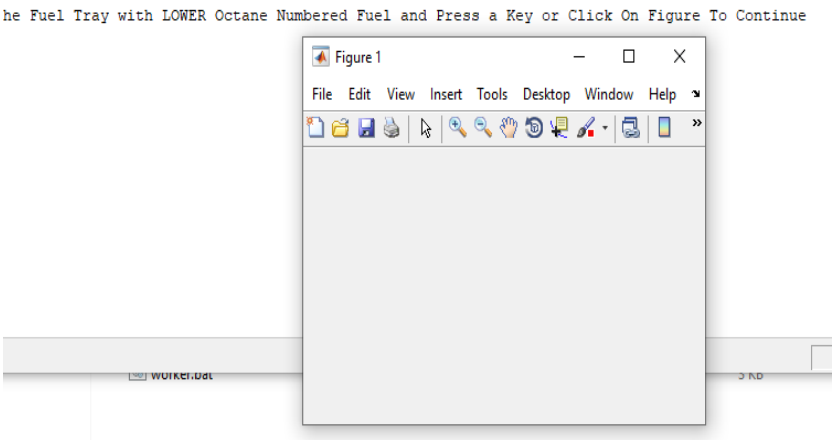


*Figure B.1.* Fuel Change Warning

- As it is described in warning area, fuel tray is filled with the lower octane numbered reference fuel. Until user press a key or click to figure, software does not perform any data collection or calculation.
- After fuel type changed, CFR engine run with the new fuel to clean up fuel hoses, carburetor and reach steady state.
- To reach maximum knock intensity same procedure is followed as the former reference fuel. Without changing the compression ratio, carburetor needle and air fuel ratio adjusted according to maximum knock intensity.
- Same data collection procedure applicable for second reference fuel. As it is stated in 21-25. Array G in the code contains voltage data
- When data collecting finishes, secondary warning occurs for the fuel with the unknown octane number.

- Same steps again repeat for the fuel with the unknown octane number. However, CFR engine procedure is slightly different because LPG is not liquid and pressurized tank used instead of fuel tray. LPG tank is connected to fuel hose via tank connector. When CFR engine starts with LPG there should be any liquid reference fuel inside the. Otherwise, carburetor sends both fuel inside the combustion chamber and result in very different octane rating. Moreover, carburetor needle cannot be used to adjust air fuel ratio. LGP valve which located on the fuel hose should be used instead.
- After all data collected for there of fuels, engine run without a fuel to cool it down for 5 minutes.
- Engine ignition switch turned off.
- CFR engine stopped.

## C. Modified and Original Piston Drawing

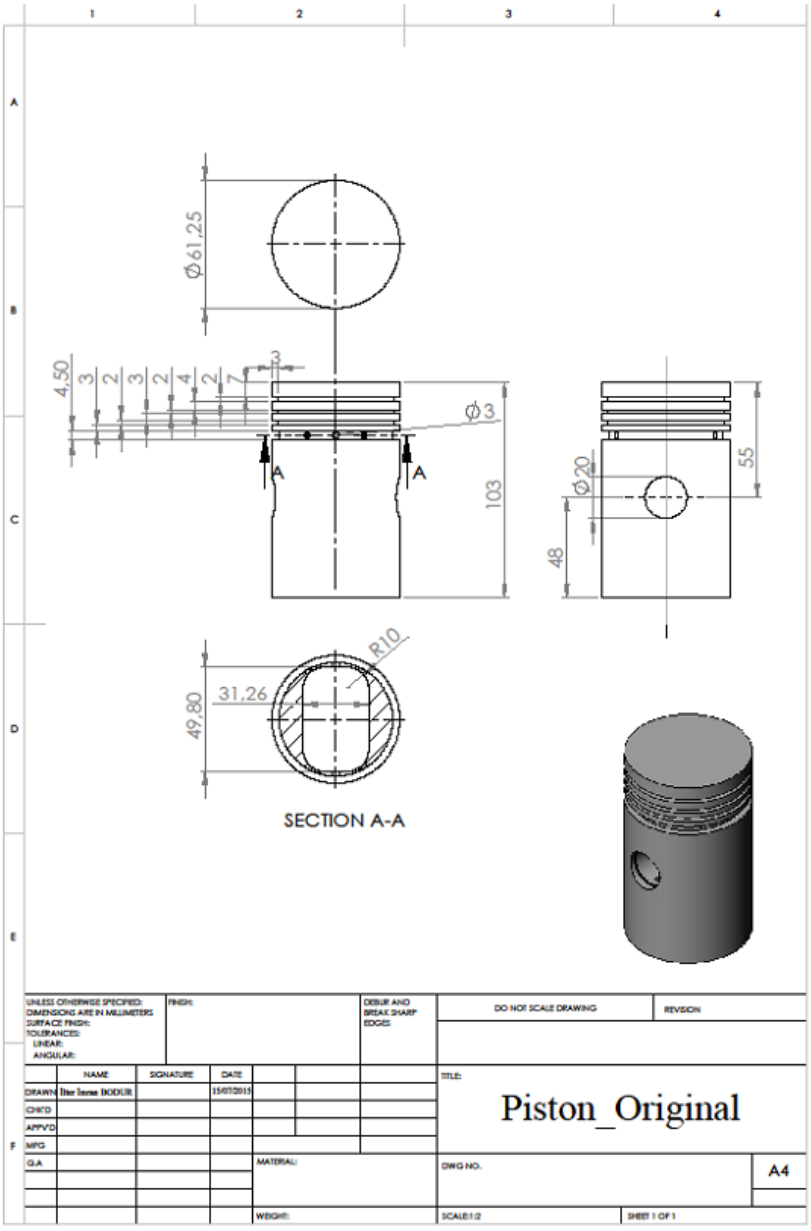


*Figure C.1.* Standard Engine Piston of CFR Engine

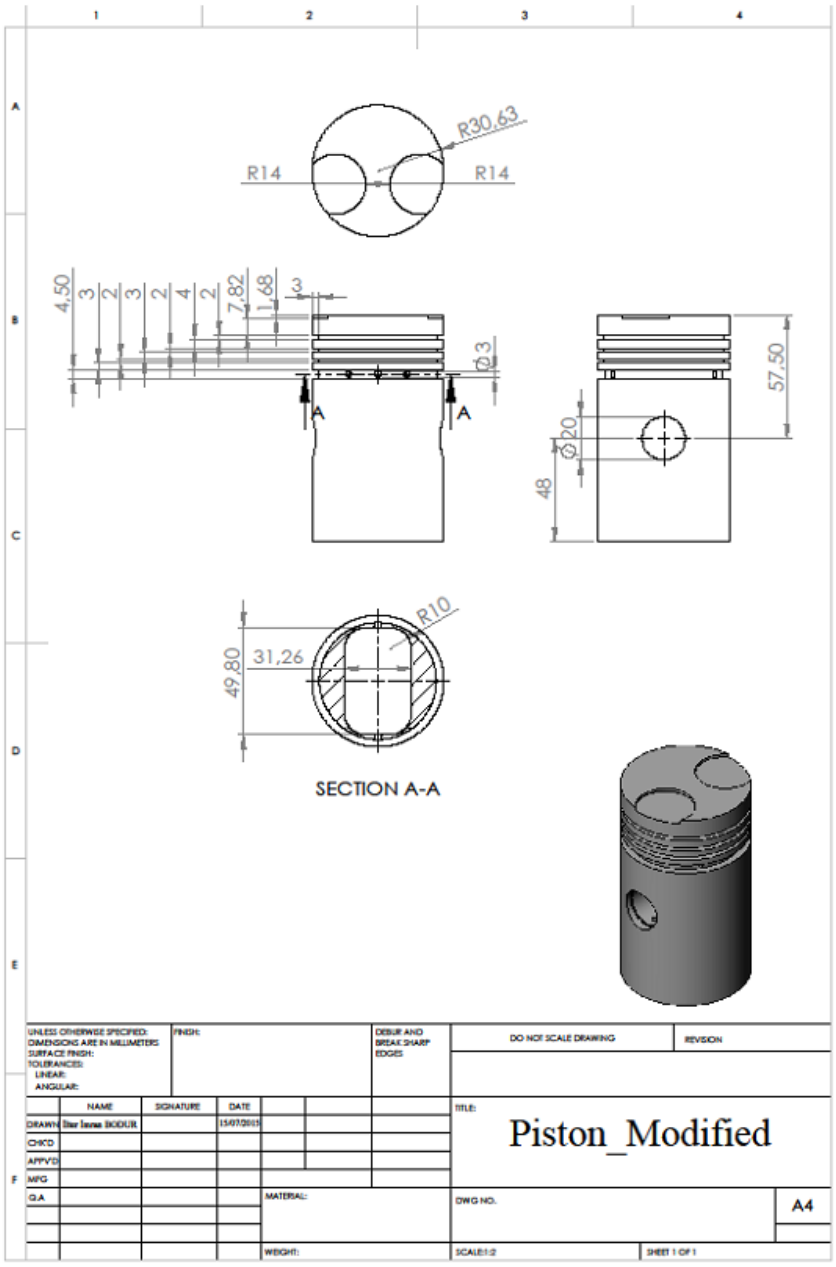


*Figure C.2.* Modified Piston of CFR Engine